Bayesian posteriors of uncertainty quantification in computational structural dynamics for low- and medium-frequency ranges

Christian Soize

Bayesian posteriors of uncertainty quantification in computational structural dynamics for low- and medium-frequency ranges

C. Soize*[a]

[a] *Université Paris-Est, Laboratoire Modélisation et Simulation Multi-Echelle, MSME UMR 8208 CNRS, 5 bd Descartes, 77454 Marne-la-Vallee, France*

Abstract

The paper is devoted to the modeling and identification of uncertainties in computational structural dynamics for low- and medium-frequency ranges. A complete methodology is presented for the identification procedure. The first eigenfrequencies are used to quantify the uncertainties in the low-frequency band while the frequency response functions are used to quantify the uncertainties in the medium-frequency band. The system-parameter uncertainties are taken into account with the parametric probabilistic approach. The model uncertainties are taken in to account with the nonparametric probabilistic approach. The posterior stochastic model of system-parameter uncertainties is identified using the Bayes method.

Keywords: uncertainty quantification, computational dynamics, medium frequency, identification, statistical inverse methods, prior stochastic model, posterior stochastic model, Bayes method, nonparametric

1. Introduction

This paper deals with the development of a methodology devoted to the identification of stochastic models of uncertainties in linear *computational structural dynamics* for the low- and medium-frequency ranges. The computational model is a second-order linear differential equation in the time domain, constructed by using the finite element method and which is analyzed in the frequency domain taking the Fourier transform. The system-parameter uncertainties are taken into account with the *parametric* probabilistic approach while the modeling errors are taken into account with the *nonparametric* probabilistic approach. A methodology which is based on the use of the maximum likelihood method is then presented for the identification of the optimal *prior* stochastic models of both the system-parameter uncertainties and the model uncertainties induced by modeling errors. The available experimental Frequency Response Functions (FRF) are used in the medium-frequency band while the first experimental eigenfrequencies are used in the low-frequency band. It is assumed that the experimental FRF are estimated with the usual spectral analysis for stationary stochastic processes of the experimental data, in presence of extraneous input and output noise. This type of estimation, based on the use of the cross-spectral

*Corresponding author
Email address: christian.soize@univ-paris-est.fr (C. Soize*)

density functions of the input and the output stationary stochastic processes, allows the effects of the extraneous noises to be removed and consequently, the experimental FRF which are estimated in presence of measurement errors, do not depend of these noises [13, 14]. The first experimental eigenfrequencies are deduced from the experimental FRF over all the frequency band. The *posterior* stochastic model of system-parameter uncertainties, in presence of modeling errors, is constructed using the first experimental eigenfrequencies in the low-frequency band and the *Bayes method*. The methodology proposed is validated with a numerical application. It should be noted that the novel methodology proposed uses classical tools and is the result of a compromise between the speed of convergence of the statistical estimators and all the others considerations related to the ease of implementation in commercial software devoted to computational mechanics (intrusive or non intrusive methods), ease of development in software, numerical cost in taking into account increasing trend of computer power and ease of parallelization of the algorithms.

2. Short overview on stochastic modeling of uncertainties whose stochastic models have to be identified and related topics

2.1. Uncertainty and variability

The designed system is used to manufacture the real system and to construct the nominal computational model (also called the mean computational model or sometimes, the mean model) using a mathematical-mechanical modeling process for which the main objective is the prediction of the responses of the real system in its environment. The real system, submitted to a given environment, can exhibit a variability in its responses due to fluctuations in the manufacturing process and due to small variations of the configuration around a nominal configuration associated with the designed system. The mean (or nominal) computational model which results from a mathematical-mechanical modeling process of the design system, exhibits parameters which can be uncertain. In this case, there are uncertainties on the computational model parameters (also called below, system-parameter uncertainties). On the other hand, the modeling process induces some modeling errors defined as the model uncertainties. It is important to take into account both the uncertainties on the system parameters and the modeling errors in order to improve the predictions of the computational model which allows robust optimization, robust design and robust updating with respect to uncertainties to be carried out.

2.2. Types of approaches for constructing prior stochastic models of uncertainties

Several approaches can be used to take into account uncertainties in computational models. The main approaches are based on the intervals method, the fuzzy logic and the probability theory. For a recent overview concerning these approaches, we refer the reader to [34]. In this paper, only the probability theory will be considered.

The parametric probabilistic approach consists in modeling the uncertain parameters of the computational model by random variables and then in constructing the stochastic model of these random variables. Many works have been published and a state-of-the-art can be found, for instance, in [30, 37, 46, 62, 63, 64, 66, 67, 79]. Concerning model uncertainties induced by modeling errors, it is today well understood that the stochastic models of the uncertain parameters of the computational model are not sufficient and have not the capability to take into account model uncertainties [9, 70]. Two main methods can be used to take into account modeling errors.

(i) The first one consists in introducing a stochastic model of the output-prediction-error method, considered as a noise, which is the difference between the real system output and the computational model output [9]. It should be noted that this method has been extended [12] to cover both the uncertainties on the system parameters of the computational model using the usual parametric probabilistic approach and the modeling errors using the output-prediction-error approach. The output-prediction-error method is certainly efficient to take into account modeling errors if a lot of experimental data is available. In contrast, if no experimental data are available, then this "global" method cannot be used to construct a family of prior stochastic models of modeling errors in structural dynamics because, generally, there are no significant information for constructing such a family for the output-prediction errors (the noise). In addition, the output-prediction-error method, considered as a stochastic modeling of modeling errors, does not allow the different sources of modeling errors and the measurements errors to be separately identified in the sense explained hereinafter. For complex dynamical systems, the complex structure must often be considered as an assemblage of substructures for which the level of modeling errors is different from a substructure to another one (nonhomogeneous modeling errors in the complex structure) and can also have different levels of modeling errors for the boundary conditions and for the coupling between the substructures. The output-prediction-error method is not adapted for constructing a family of prior stochastic models of modeling errors for such complex dynamical systems for which we are interested in constructing a family of prior stochastic models of modeling errors for each operator of the dynamical system: mass, damping and stiffness operators for each substructure, boundary operators, coupling operators between substructures, each operator having its own algebraic properties and its own level of modeling errors. It should be noted that the parametric probabilistic approach of system-parameter uncertainties cannot be used to represent such modeling errors on these operators as previously explained. If there is no available experimental data, an adapted family of prior stochastic models of modeling errors must be constructed and used to perform a robust analysis with respect to the level of modeling errors for the different parts of the complex dynamical systems. For limited experimental data, the quality and the capability of such prior stochastic models of modeling errors plays a very important role. In this framework of uncertain complex dynamical systems and if only limited experimental data are available, the output-prediction-error method is not really adapted.

(ii) The second one is based on the nonparametric probabilistic approach of model uncertainties induced by modeling errors, which has been proposed in [70, 71] as an alternative method to the output-prediction-errors method in order to take into account modeling errors at the operators level by introducing random operators and not at the computational model output level by introducing an additive noise. With such an approach, the stochastic model of the modeling errors and the stochastic model of the measurement errors can separately be identified [79]. As used in this paper, uncertainties on the system parameters and the modeling errors can be taken into account using simultaneously the parametric probabilistic approach of system-parameter uncertainties and the nonparametric probabilistic approach of modeling errors [78]. The fundamental difference between the output-prediction-error method and the nonparametric probabilistic method, to take into account modeling errors in computational structural dynamics, is the choice of the parametrization of modeling errors. For the output-prediction-error method, an additive noise is added in the output. For the nonparametric probabilistic approach, the different sources of modeling errors are taken into account at the levels of the operators of the dynamical system. If no experimental data are available, the first method is not appropriate to construct a family of prior stochastic models of modeling errors while the second one is appropriate. The non-

parametric probabilistic approach is based on the use of a reduced-order model and the random matrix theory. It consists in directly constructing the stochastic model of the operators of the mean (or nominal) computational model. In addition, the nonparametric probabilistic approach of modeling errors is adapted and has been validated to take into account

- nonhomogeneous modeling errors in the complex structure described as an assemblage of substructures with different levels of modeling errors [23, 32, 36];
- modeling errors in the boundary conditions and in the coupling between the substructures, independently from the other sources of modeling errors [51, 52];
- modeling errors for nonlinear dynamical systems with geometrical nonlinearity in three-dimensional elasticity [53, 21] and with nonlinear constitutive equation [61].

Since the paper [70], many works have been published, in particular concerning extension of the theory and its experimental validations [5, 7, 8, 17, 18, 23, 24, 29, 31, 32, 33, 36, 42, 50, 60, 61, 72, 73, 74, 76, 78, 79].

2.3. Uncertainty quantification and identification of the stochastic models of uncertainties

The main statistical tools which are useful to identify the stochastic model of uncertainties using experimental data are mainly the least-square method, the maximum likelihood method [68, 81, 86] and the Bayes method [15, 22, 28, 41, 47, 81, 84]. Many works have been published in the field of statistical inverse methods and their applications. In the context of uncertain mechanical and dynamical systems, we refer the reader, for instance, to [9, 11, 12, 25, 26, 27, 39, 43, 83, 84]. Among all these works, it should be noted that a Bayesian computational method is presented in [11] for calculating a stochastic prediction, based on the use of Markov Chain Monte Carlo (MCMC) methods for computing integrals in high dimension. Such MCMC method can be developed in introducing a stochastic dissipative Hamiltonian system such as introduced in [75] and in [25, 26]. Concerning the experimental identification of the parameters of the prior probability distributions of random matrices introduced by the nonparametric probabilistic approach of uncertainties in computational mechanics, we refer the reader to [5, 6, 7, 8, 23, 24, 32, 33, 36, 74, 76, 78]. The statistical inverse methods and the Bayesian inference approach to inverse problems have received a particular attention [9, 11, 12, 25, 26, 27, 35, 45, 48, 79, 87, 88, 90].

2.4. Comments concerning robust updating and robust design

Robust updating or robust design optimization consists in updating a computational model or in optimizing the design of a mechanical system with a computational model, in taking into account both the system-parameter uncertainties and the modeling errors. When experimental data are available, the identification of the stochastic models of uncertainties in the computational model plays an important role for getting the necessary robustness. An overview on computational methods in optimization considering uncertainties can be found in [65]. Robust updating and robust design developments with uncertain system parameters can be found in [10, 38, 57, 58, 59, 82] while robust updating or robust design optimization with modeling errors taken into account with nonparametric probabilistic approach can be found in [19, 20, 61, 77].

3. Short overview on parametric and nonparametric stochastic models in computational structural dynamics for low- and medium-frequency ranges

3.1. Introduction of the mean computational model in linear structural dynamics

The dynamical system is a damped fixed structure around a static equilibrium configuration considered as a natural state without prestresses and subjected to an external load. The dynamical system is analyzed in the frequency band $\mathcal{B} =]0\,, \omega_{\max}]$ and the generic point in $\mathcal{B}$ is denoted by ω in rad/s. It is assumed that a set of system parameters has been identified as the uncertain system parameters which are the components of a vector $\mathbf{x} = (x_1, \ldots, x_{n_p})$ belonging to an admissible set C_{par} which is a subset of $\mathbb{R}^{n_p}$. Using the finite element method to construct a finite approximation of the boundary value problem yields the dynamical equation of the *mean* (or *nominal*) computational model, which is written in the frequency domain, for all ω in $\mathcal{B}$, as

$$(-\omega^2[\,\mathbb{M}(\mathbf{x})] + i\omega\,[\,\mathbb{D}(\mathbf{x})] + [\,\mathbb{K}(\mathbf{x})])\,\mathbb{y}(\omega) = \mathbb{f}(\omega; \mathbf{x}), \tag{1}$$

in which $i = \sqrt{-1}$, where $\mathbb{y}(\omega)$ is the complex frequency response vector of the m degrees of freedom (DOF) (displacements and/or rotations), where $\mathbb{f}(\omega; \mathbf{x})$ is the external load vector of the m inputs (forces and/or moments) and finally, where $[\,\mathbb{M}(\mathbf{x})]$, $[\,\mathbb{D}(\mathbf{x})]$ and $[\,\mathbb{K}(\mathbf{x})]$ are the mass, damping and stiffness matrices of the mean computational model, which belong to the set $\mathbb{M}^+_m(\mathbb{R})$ of all the positive-definite symmetric $(m \times m)$ real matrices. In order to not increase the complexity of notations, the dependency in $\mathbf{x}$ of the response is removed. In this paper which is devoted to the Bayesian posteriors of uncertainty quantification, it is assumed that the damping and stiffness matrices are independent of ω. Nevertheless, in the medium-frequency range, these matrices can depend on the frequency and it can be necessary to take into account the viscoelastic behavior of the structure (see for instance [55]). In such a case, the nonparametric probabilistic approach of uncertainties can also be used as explained in [74, 79] or in using the new extension for viscoelastic structure as recently proposed in [56, 80].

3.2. Construction of the reduced-order mean computational model

(i) - Remarks on two approaches for constructing the reduced-order model. In the context of linear structural dynamics, two main approaches can be used.

(i-1) The first one consists in calculating the elastic modes for $\mathbf{x}$ fixed to its nominal value $\underline{\mathbf{x}} = (\underline{x}_1, \ldots, \underline{x}_{n_p})$. We then obtain the elastic modes of the nominal mean computational model which are independent of $\mathbf{x}$ and which depend only on $\underline{\mathbf{x}}$. In this case, when $\mathbf{x}$ runs through C_{par}, matrices $[\,\mathbb{M}(\mathbf{x})]$ and $[\,\mathbb{K}(\mathbf{x})]$ have to be projected on the subspace spanned by the elastic modes of the nominal mean computational model. This approach does not require reanalyzes but the projection of the matrices depending on $\mathbf{x}$ is intrusive with respect to the usual commercial softwares which often are black boxes.

(i-2) The second one consists in calculating the elastic modes for each required $\mathbf{x}$ belonging to C_{par}. In this case, the elastic modes of the mean computational model depend on $\mathbf{x}$. In the context of the parametric probabilistic approach of system-parameter uncertainties, we then have to solve a random generalized eigenvalue problem and such an approach is better adapted to usual commercial softwares and allows a fast convergence to be obtained with respect to the dimension of the reduced-order model. This approach is not intrusive but in counter part requires reanalyzes. Nevertheless, these reanalyzes can easily be parallelized without any software development and

in addition, we will see how the numerical cost can be decreased at the end of the following paragraph (ii).

(ii) - Reduced-order model constructed with the second approach. Below, for sake of brevity, we limit the developments to the first apprach, but clearly the second one could be used. For all $\mathbf{x}$ fixed in C_{par}, let $\{\boldsymbol{\phi}_1(\mathbf{x}), \ldots, \boldsymbol{\phi}_m(\mathbf{x})\}$ be the algebraic basis of $\mathbb{R}^m$ constructed with the elastic modes. For each selected $\mathbf{x}$ in C_{par}, these elastic modes are solution of the generalized eigenvalue problem

$$[\,\mathbb{K}(\mathbf{x})]\,\boldsymbol{\phi}_\alpha(\mathbf{x}) = \lambda_\alpha(\mathbf{x})\,[\,\mathbb{M}(\mathbf{x})]\,\boldsymbol{\phi}_\alpha(\mathbf{x})\,, \tag{2}$$

for which the eigenfrequencies

$$0 < \omega_1(\mathbf{x}) \leq \omega_2(\mathbf{x}) \leq \ldots \leq \omega_m(\mathbf{x})\,, \tag{3}$$

with $\omega_\alpha(\mathbf{x}) = \sqrt{\lambda_\alpha(\mathbf{x})}$ and the associated elastic modes $\{\boldsymbol{\phi}_1(\mathbf{x}), \boldsymbol{\phi}_2(\mathbf{x}), \ldots\}$ are such that

$$<[\,\mathbb{M}(\mathbf{x})]\,\boldsymbol{\phi}_\alpha(\mathbf{x})\,, \boldsymbol{\phi}_\beta(\mathbf{x})> = \mu_\alpha(\mathbf{x})\,\delta_{\alpha\beta}\,, \tag{4}$$

$$<[\,\mathbb{K}(\mathbf{x})]\,\boldsymbol{\phi}_\alpha(\mathbf{x})\,, \boldsymbol{\phi}_\beta(\mathbf{x})> = \mu_\alpha(\mathbf{x})\,\omega_\alpha(\mathbf{x})^2\,\delta_{\alpha\beta}\,, \tag{5}$$

in which the brackets denote the Euclidean inner product. For each value of $\mathbf{x}$ given in C_{par}, the reduced-order mean computational model of the dynamical system is obtained in constructing the projection of the mean computational model on the subspace spanned by $\{\boldsymbol{\phi}_1(\mathbf{x}), \ldots, \boldsymbol{\phi}_n(\mathbf{x})\}$ with $n \ll m$. Let $[\,\phi(\mathbf{x})]$ be the $(m \times n)$ real matrix whose columns are vectors $\{\boldsymbol{\phi}_1(\mathbf{x}), \ldots, \boldsymbol{\phi}_n(\mathbf{x})\}$. The generalized force $\mathbf{f}(\omega; \mathbf{x})$ is a $\mathbb{C}^n$-vector such that $\mathbf{f}(\omega; \mathbf{x}) = [\,\phi(\mathbf{x})]^T\,\mathbb{f}(\omega; \mathbf{x})$. For all $\mathbf{x}$ in C_{par}, the generalized mass, damping and stiffness matrices $[M(\mathbf{x})]$, $[D(\mathbf{x})]$ and $[K(\mathbf{x})]$ belong to $\mathbb{M}^+_n(\mathbb{R})$ and are defined by

$$[M(\mathbf{x})]_{\alpha\beta} = \mu_\alpha(\mathbf{x})\,\delta_{\alpha\beta}\,, \tag{6}$$

$$[K(\mathbf{x})]_{\alpha\beta} = \mu_\alpha(\mathbf{x})\,\omega_\alpha(\mathbf{x})^2\,\delta_{\alpha\beta}\,, \tag{7}$$

$$[D(\mathbf{x})]_{\alpha\beta} = <[\,\mathbb{D}(\mathbf{x})]\,\boldsymbol{\phi}_\beta(\mathbf{x})\,, \boldsymbol{\phi}_\alpha(\mathbf{x})>\,, \tag{8}$$

in which, generally, $[D(\mathbf{x})]$ is a full matrix. Consequently, for all $\mathbf{x}$ in C_{par} and for all fixed ω, the reduced-order mean computational model of the dynamical system is written as the projection $\mathbf{y}^n(\omega)$ of $\mathbb{y}(\omega)$ such that $\mathbf{y}^n(\omega) = [\,\phi(\mathbf{x})]\,\mathbf{q}(\omega)$ in which $\mathbf{q}(\omega)$ is the $\mathbb{C}^n$-vector of the generalized coordinates. The reduced-order mean computational model is then written, for all ω in $\mathcal{B}$, as

$$\mathbf{y}^n(\omega) = [\,\phi(\mathbf{x})]\,\mathbf{q}(\omega)\,, \tag{9}$$

$$(-\omega^2[M(\mathbf{x})] + i\omega\,[D(\mathbf{x})] + [K(\mathbf{x})])\mathbf{q}(\omega) = \mathbf{f}(\omega; \mathbf{x})\,. \tag{10}$$

Below, we will denote by n_0 the value of n for which the response $\mathbf{y}^n$ is converged to $\mathbb{y}$, with a given accuracy, for all ω in $\mathcal{B}$ and for all the values of $\mathbf{x}$ in C_{par}. As we will see, for the identification procedure of the prior and the posterior stochastic models, the methodology proposed is based on the use of a sampling technique of random quantities. It should be noted that such a choice is independent of the method used for solving the stochastic linear equation associated with Eq. (1) or solving the stochastic reduced-order model associated with Eqs. (9)-(10). The stochastic solver can either be based on a sampling technique (Monte Carlo method), or be based on a spectral method (Galerkin approach for the probability space) using, for instance, the polynomial chaos expansion [37, 44, 54]. In such a case, the independent realizations (sampling technique) of the random quantities can easily be generated from the polynomial chaos expansion.

Therefore, as soon as the sampling technique is used for the random quantities, in particular, for the prior stochastic model of $\mathbf{x}$, a finite family of sampling points $\mathbf{x}(\theta_1), \ldots, \mathbf{x}(\theta_{\nu_p})$ can be calculated and thus, the generalized eigenvalue problem is solved for these sampling points. If the dimension n_p of the uncertain vector $\mathbf{x}$ is sufficiently small, the computational cost can be reduced for constructing the following ν_p quintuplets $\{[M(\mathbf{x}(\theta_j))], [D(\mathbf{x}(\theta_j))], [K(\mathbf{x}(\theta_j))], [\phi(\mathbf{x}(\theta_j))], [Z(\mathbf{x}(\theta_j))]\}$ with $[Z(\mathbf{x}(\theta_j))] = [M(\mathbf{x}(\theta_j))][\phi(\mathbf{x}(\theta_j))]$ in using the interpolating method on manifolds proposed in [1, 2, 3].

3.3. Construction of the prior stochastic model of system-parameter uncertainties

The parametric probabilistic approach of system-parameter uncertainties consists in modeling the uncertain system parameter $\mathbf{x}$ (whose nominal value is $\underline{\mathbf{x}}$) by a random variable $\mathbf{X}$ defined on a probability space $(\Theta, \mathcal{T}, \mathcal{P})$, with values in $\mathbb{R}^{n_p}$. The prior probability distribution of $\mathbf{X}$ is assumed to be defined by a probability density function (pdf) $p_{\mathbf{X}}^{\text{prior}}$ on $\mathbb{R}^{n_p}$. The prior model can be constructed using the maximum entropy principle [40, 69, 75] for which the available information is defined as follows. Since $\mathbf{x}$ belongs to C_{par}, the support of $p_{\mathbf{X}}^{\text{prior}}$ must be C_{par} and the normalization condition must be verified. Since the nominal value of $\mathbf{x}$ is $\underline{\mathbf{x}} \in C_{\text{par}}$, we have $E\{\mathbf{X}\} = \underline{\mathbf{x}}$. In general, an additional available information can be deduced from the analysis of the mathematical properties of the solution of the stochastic reduced-order computational model under construction which yields an additional vector-valued constraint defined by a vectorial equation of dimension μ_X. The solution $p_{\mathbf{X}}^{\text{prior}}$ of the maximum entropy principle then depends on the free $\mathbb{R}^{\mu_X}$-valued parameter related to the additional vector-valued constraint which is written as a function of a $\mathbb{R}^{\mu_X}$-valued parameter $\boldsymbol{\delta}_X$ which corresponds to a well defined statistical quantity for random variable $\mathbf{X}$, such as the coefficients of variation of its components. In general, $\boldsymbol{\delta}_X$ does not run through $\mathbb{R}^{\mu_X}$ but must belong to an admissible set C_X which is a subset of $\mathbb{R}^{\mu_X}$. Consequently, $p_{\mathbf{X}}^{\text{prior}}$ depends on $\underline{\mathbf{x}}$ and $\boldsymbol{\delta}_X$ and we will write this prior pdf as

$$\mathbf{x} \mapsto p_{\mathbf{X}}^{\text{prior}}(\mathbf{x}; \underline{\mathbf{x}}, \boldsymbol{\delta}_X) \quad \text{with} \quad (\underline{\mathbf{x}}, \boldsymbol{\delta}_X) \in C_{\text{par}} \times C_X \,. \tag{11}$$

3.4. Construction of the prior stochastic model of model uncertainties induced by modeling errors

The nonparametric probabilistic approach [70, 71, 74] is used to take into account the model uncertainties induced by modeling errors. Let $(\Theta', \mathcal{T}', \mathcal{P}')$ be another probability space. For n fixed to the value n_0 and for all $\mathbf{x}$ fixed in C_{par}, the nonparametric probabilistic approach of modeling errors consists in replacing, in Eq. (10), the matrices $[M(\mathbf{x})]$, $[D(\mathbf{x})]$ and $[K(\mathbf{x})]$ by the random matrices

$$\begin{aligned} [\mathbf{M}(\mathbf{x})] &= \{\theta' \mapsto [\mathbf{M}(\theta'; \mathbf{x})]\} \,, \\ [\mathbf{D}(\mathbf{x})] &= \{\theta' \mapsto [\mathbf{D}(\theta'; \mathbf{x})]\} \,, \\ [\mathbf{K}(\mathbf{x})] &= \{\theta' \mapsto [\mathbf{K}(\theta'; \mathbf{x})]\} \,, \end{aligned} \tag{12}$$

defined on probability space $(\Theta', \mathcal{T}', \mathcal{P}')$, depending on parameter $\mathbf{x}$ and such that $E\{[\mathbf{M}(\mathbf{x})]\} = [M(\mathbf{x})]$, $E\{[\mathbf{D}(\mathbf{x})]\} = [D(\mathbf{x})]$ and $E\{[\mathbf{K}(\mathbf{x})]\} = [K(\mathbf{x})]$. These random matrices are written as

$$\begin{aligned} [\mathbf{M}(\mathbf{x})] &= [L_M(\mathbf{x})]^T \, [\mathbf{G}_M] \, [L_M(\mathbf{x})] \,, \\ [\mathbf{D}(\mathbf{x})] &= [L_D(\mathbf{x})]^T \, [\mathbf{G}_D] \, [L_D(\mathbf{x})] \,, \\ [\mathbf{K}(\mathbf{x})] &= [L_K(\mathbf{x})]^T \, [\mathbf{G}_K] \, [L_K(\mathbf{x})] \,, \end{aligned} \tag{13}$$

in which $[L_M(\mathbf{x})]$, $[L_D(\mathbf{x})]$ and $[L_K(\mathbf{x})]$ are the upper triangular matrices such that

$$\begin{aligned} [M(\mathbf{x})] &= [L_M(\mathbf{x})]^T\,[L_M(\mathbf{x})]\,, \\ [D(\mathbf{x})] &= [L_D(\mathbf{x})]^T\,[L_D(\mathbf{x})]\,, \\ [K(\mathbf{x})] &= [L_K(\mathbf{x})]^T\,[L_K(\mathbf{x})]\,, \end{aligned} \tag{14}$$

and where $[\mathbf{G}_M]$, $[\mathbf{G}_D]$ and $[\mathbf{G}_K]$ are statistically independent random matrices, defined on probability space $(\Theta', \mathcal{T}', \mathcal{P}')$, with values in $\mathbb{M}_n^+(\mathbb{R})$, and which belong to $\mathrm{SG}_\varepsilon^+$ defined in Appendix A.2. These three random matrices depend on the dispersion parameter $\boldsymbol{\delta}_G = (\delta_M, \delta_D, \delta_K)$ which allows the level of model uncertainties to be controlled and which belongs to an admissible set $C_G \subset \mathbb{R}^3$. Consequently, the prior joint pdf of random matrices $[\mathbf{G}_M]$, $[\mathbf{G}_D]$ and $[\mathbf{G}_K]$ is written, for $\boldsymbol{\delta}_G$ in $C_G \subset \mathbb{R}^3$, as

$$([G_M],[G_D],[G_K]) \mapsto p_{\mathbf{G}}^{\text{prior}}([G_M],[G_D],[G_K];\boldsymbol{\delta}_G), \tag{15}$$

and which is the product of $p_{[\mathbf{G}_M]}([G_M];\delta_M)$, $p_{[\mathbf{G}_D]}([G_D];\delta_D)$ and $p_{[\mathbf{G}_K]}([G_K];\delta_K)$, each one of these pdf being deduced from Eq. (**??**). The algebraic representations of random matrices $[\mathbf{G}_M]$, $[\mathbf{G}_D]$ and $[\mathbf{G}_K]$, which are useful for generating independent realizations $[\mathbf{G}_M(\theta')]$, $[\mathbf{G}_D(\theta')]$ and $[\mathbf{G}_K(\theta')]$, are explicitly defined, using Eq. (A.2) and the algebraic representation of random matrix $[\mathbf{G}_0]$ defined in Appendix A.1.

3.5. Construction of the stochastic reduced-order computational model with the prior stochastic models of uncertainties

Dimension n is fixed to the value n_0. The reduced-order mean computational model, defined by Eqs. (9) and (10), is then replaced by the following stochastic reduced-order computational model,

$$\mathbf{Y}(t) = [\,\phi(\mathbf{X})]\,\mathbf{Q}(t)\,, \tag{16}$$

$$(-\omega^2[\mathbf{M}(\mathbf{X})] + i\omega[\mathbf{D}(\mathbf{X})] + [\mathbf{K}(\mathbf{X})])\mathbf{Q}(\omega) = \mathbf{f}(\omega;\mathbf{X}), \tag{17}$$

in which for all fixed ω, $\mathbf{Y}(\omega) = \{(\theta,\theta') \mapsto \mathbf{Y}(\theta,\theta';\omega)\}$ and $\mathbf{Q}(\omega) = \{(\theta,\theta') \mapsto \mathbf{Q}(\theta,\theta';\omega)\}$ are $\mathbb{C}^m$- and $\mathbb{C}^n$-valued random vectors defined on $\Theta \times \Theta'$. It is assumed that the prior stochastic modeling is such that, for all ω in $\mathcal{B}$, Eq. (17) admits a second-order random solution $\mathbf{Q}(\omega)$.

Below, the following notations are used. Any realization of random variable $\mathbf{X}$ is denoted by $\mathbf{X}(\theta_\ell)$ for θ_ℓ in Θ. For all $\mathbf{x}$ in C_{par}, any realizations of random matrices $[\mathbf{M}(\mathbf{x})]$, $[\mathbf{D}(\mathbf{x})]$, $[\mathbf{K}(\mathbf{x})]$ are denoted by $[\mathbf{M}(\theta'_{\ell'};\mathbf{x})]$, $[\mathbf{D}(\theta'_{\ell'};\mathbf{x})]$ and $[\mathbf{K}(\theta'_{\ell'};\mathbf{x})]$ for $\theta'_{\ell'}$ in Θ'.

(i) Realization of the first random eigenfrequencies. A realization

$$0 < \Omega_1(\theta_\ell,\theta'_{\ell'}) \leq \ldots \leq \Omega_{N_{\text{eig}}}(\theta_\ell,\theta'_{\ell'}) \tag{18}$$

of the first N_{eig} random eigenfrequencies of the associated stochastic conservative system are such that, for $\alpha = 1,\ldots,N_{\text{eig}}$,

$$\begin{aligned} &[\mathbf{K}(\theta'_{\ell'};\mathbf{X}(\theta_\ell))]\,\mathbf{Q}^\alpha(\theta_\ell,\theta'_{\ell'}) = \\ &\qquad \Omega_\alpha(\theta_\ell,\theta'_{\ell'})^2\,[\mathbf{M}(\theta'_{\ell'};\mathbf{X}(\theta_\ell))]\,\mathbf{Q}^\alpha(\theta_\ell,\theta'_{\ell'})\,. \end{aligned} \tag{19}$$

(ii) - Realization of the stochastic reduced-order system for both the system-parameter uncertainties and the model uncertainties. The realizations

$$\mathbf{y}_{\ell,\ell'}(\omega) = \mathbf{Y}(\theta_\ell, \theta'_{\ell'}; \omega) \ , \ \mathbf{q}_{\ell,\ell'}(\omega) = \mathbf{Q}(\theta_\ell, \theta'_{\ell'}; \omega) \tag{20}$$

of random variables $\mathbf{Y}(\omega)$ and $\mathbf{Q}(\omega)$ verify the following deterministic equations

$$\mathbf{y}_{\ell,\ell'}(\omega) = [\, \phi(\mathbf{X}(\theta_\ell))] \, \mathbf{q}_{\ell,\ell'}(\omega) \,, \tag{21}$$

$$\begin{aligned}(-\omega^2[\mathbf{M}(\theta'_{\ell'}; \mathbf{X}(\theta_\ell))] + i\omega\,[\mathbf{D}(\theta'_{\ell'}; \mathbf{X}(\theta_\ell))] \\ +[\mathbf{K}(\theta'_{\ell'}; \mathbf{X}(\theta_\ell))]) \, \mathbf{q}_{\ell,\ell'}(\omega) = \mathbf{f}(\omega; \mathbf{X}(\theta_\ell)) \,.\end{aligned} \tag{22}$$

(iii) - Realization of the stochastic reduced-order system for deterministic system parameter and model uncertainties. For this case, the system parameter is equal to the deterministic nominal vector $\mathbf{X} = \underline{\mathbf{x}}$ and $\delta_X = 0$. Let $[\mathbf{M}(\theta'_{\ell'}; \underline{\mathbf{x}})]$, $[\mathbf{D}(\theta'_{\ell'}; \underline{\mathbf{x}})]$ and $[\mathbf{K}(\theta'_{\ell'}; \underline{\mathbf{x}})]$ be any realizations of random matrices $[\mathbf{M}(\underline{\mathbf{x}})]$, $[\mathbf{D}(\underline{\mathbf{x}})]$, $[\mathbf{K}(\underline{\mathbf{x}})]$ for $\theta'_{\ell'}$ in Θ'. The realizations

$$\mathbf{y}_{\ell'}(\omega) = \mathbf{Y}(\theta'_{\ell'}; \omega) \ , \ \mathbf{q}_{\ell'}(\omega) = \mathbf{Q}(\theta'_{\ell'}; \omega) \tag{23}$$

of random variables $\mathbf{Y}(\omega)$ and $\mathbf{Q}(\omega)$ verify the following deterministic equations

$$\mathbf{y}_{\ell'}(\omega) = [\, \phi(\underline{\mathbf{x}})] \, \mathbf{q}_{\ell'}(\omega) \,, \tag{24}$$

$$\begin{aligned}(-\omega^2[\mathbf{M}(\theta'_{\ell'}; \underline{\mathbf{x}})] + i\omega\,[\mathbf{D}(\theta'_{\ell'}; \underline{\mathbf{x}})] \\ +[\mathbf{K}(\theta'_{\ell'}; \underline{\mathbf{x}})]) \, \mathbf{q}_{\ell'}(\omega) = \mathbf{f}(\omega; \underline{\mathbf{x}}) \,.\end{aligned} \tag{25}$$

3.6. Stochastic solver

As we have explained above, the stochastic solver of Eqs. (16) and (17) can be based either on a sampling technique (Monte Carlo method), or on a spectral method (Galerkin approach for the probability space) using, for instance, the polynomial chaos expansion.

(1) We begin explaining the latter case and we assume that the spectral approach is based on the use of the polynomial chaos expansion. Since random matrices $[\mathbf{G}_M]$, $[\mathbf{G}_D]$ and $[\mathbf{G}_K]$ introduce a large number of random variables, it seems difficult to perform a polynomial chaos expansion with respect to $[\mathbf{G}_M]$, $[\mathbf{G}_D]$ and $[\mathbf{G}_K]$. In contrast, it is assumed that a polynomial chaos expansion can be carried out with respect to random vector $\mathbf{X}$. Consequently, the polynomial chaos expansion of random vector $\mathbf{Q}(\omega)$ defined in Eq. (17) can be written as

$$\mathbf{Q}(\omega) = \sum_\alpha \mathbf{A}^\alpha(\omega) \, \psi_\alpha(\mathbf{X}) \,, \tag{26}$$

in which $\psi_\alpha(\mathbf{x})$ are the real multi-dimensional polynomials and where $\mathbf{A}^\alpha(\omega)$ is a complex random vector (for general developments concerning the stochastic solver based on spectral approaches, see [37, 44, 54]). The family of random vector-valued coefficients, $\{\mathbf{A}^\alpha(\omega), \omega \in \mathcal{B}\}$ depends only on the modeling errors, that is to say, are defined on $(\Theta', \mathcal{T}', \mathcal{P}')$ and depends only on parameter δ_G. Consequently, using Eq. (26), the use of the sampling technique for random

vector $\mathbf{Q}(\omega)$ consists in constructing $\nu_{\rm P}$ independent realizations $\theta_1, \ldots, \theta_{\nu_{\rm P}}$ in Θ, and $\nu_{\rm NP}$ independent realizations $\theta'_1, \ldots, \theta'_{\nu_{\rm NP}}$ in Θ', such that

$$\mathbf{q}_{\ell,\ell'}(\omega) = \sum_{\alpha} \mathbf{A}^{\alpha}(\theta'_{\ell'}; \omega)\, \psi_{\alpha}(\mathbf{X}(\theta_{\ell})) \,. \tag{27}$$

From Eqs. (20) and (21), it can be deduced $\nu_{\rm P} \times \nu_{\rm NP}$ independent realizations, $\{\mathbf{y}_{\ell,\ell'}(\omega), \omega \in \mathcal{B}\}$ of the stochastic processes $\{\mathbf{Y}(\omega), \omega \in \mathcal{B}\}$. In such a case, the stochastic solution is decomposed on the polynomial chaos with respect to $\mathbf{X}$ and the realizations of the random coefficients of the polynomial chaos expansion are constructed by the Monte Carlo method which allows the realizations $\mathbf{A}^{\alpha}(\theta'_{\ell'}; \omega)$ to be directly computed.

(2) If the Monte Carlo method is used as stochastic solver, with $\nu_{\rm P}$ independent realizations $\theta_1, \ldots, \theta_{\nu_{\rm P}}$ in Θ and with $\nu_{\rm NP}$ independent realizations $\theta'_1, \ldots, \theta'_{\nu_{\rm NP}}$ in Θ', for each $(\theta_{\ell}, \theta'_{\ell'})$, the deterministic Eqs. (21) and (22) are solved for ω in $\mathcal{B}$. We then directly obtained $\nu_{\rm P} \times \nu_{\rm NP}$ independent realizations $\{\mathbf{y}_{\ell,\ell'}(\omega), \omega \in \mathcal{B}\}$ of stochastic process $\{\mathbf{Y}(\omega), \omega \in \mathcal{B}\}$. This method can also be used for Eq. (19) or for Eqs. (24) and (25).

4. Identification of parametric and nonparametric prior stochastic models of uncertainties and Bayesian posteriors for low- and medium-frequency ranges

In this section, a methodology is proposed for identifying the stochastic models of uncertainties (defined in Sections 3.3 and 3.4) in linear structural dynamics for low- and medium-frequency ranges.

4.1. Preliminary comments

The frequency band of analysis $\mathcal{B} =]0\,, \omega_{\rm max}]$ is written as $\mathcal{B} = \mathcal{B}_{\rm LF} \cup \mathcal{B}_{\rm MF}$ in which $\mathcal{B}_{\rm LF} =]0\,, \omega_{\rm min}]$ is the low-frequency band and where $\mathcal{B}_{\rm MF} =]\omega_{\rm min}\,, \omega_{\rm max}]$ is the medium-frequency band. For instance, Fig. 1 shows an example of an experimental frequency response function (in displacement) for 3 experimental configurations of a same structure. This figure clearly shows the two frequency bands for which $\omega_{\rm min}$ is about 4×10^5 Hz. The low-frequency band $\mathcal{B}_{\rm LF}$ is relatively robust with respect to uncertainties. It can be seen that variabilities are relatively small for the first six resonances, and are not significant for the first two resonances which are really robust to uncertainties. In contrast, the medium-frequency band $\mathcal{B}_{\rm MF}$ is very sensitive to uncertainties and Fig. 1 shows a large variability of the frequency response function. Such a high sensitivity of the frequency responses to uncertainties characterizes the medium-frequency range for which a stochastic modeling of uncertainties is absolutely necessary, in particular, the model uncertainties induced by modeling errors (see [20, 24, 33, 36, 42, 55, 56, 73, 76]).

4.2. Methodology for the identification

The objectives of the identification consist:
(1) in identifying the parameters $\underline{\mathbf{x}}$ and δ_X of the prior pdf $p^{\rm prior}_{\mathbf{X}}(\mathbf{x}; \underline{\mathbf{x}}, \delta_X)$ of $\mathbf{X}$ (parametric probabilistic approach of system-parameter uncertainties, see Eq. (11)), and the parameter δ_G of the prior pdf $p^{\rm prior}_{\mathbf{G}}([G_M], [G_D], [G_K]; \delta_G)$ of $[\mathbf{G}_M]$, $[\mathbf{G}_D]$, $[\mathbf{G}_K]$ (nonparametric probabilistic approach of model uncertainties induced by modeling errors, see Eq. (15)), using the maximum likelihood method and the experimental measurements. The identified values are denoted by $\underline{\mathbf{x}}^{\rm opt}, \delta_X^{\rm opt}, \delta_G^{\rm opt}$

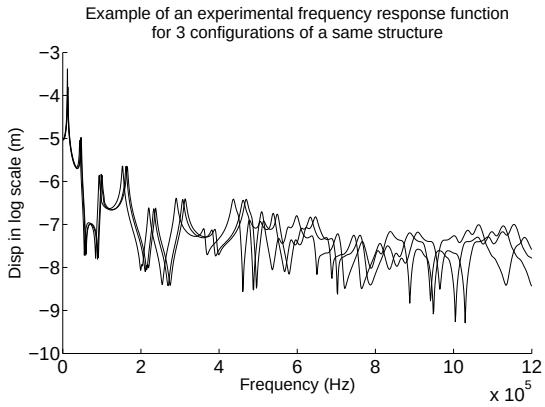

Figure 1: Low- and medium-frequency ranges: example of an experimental frequency response function for 3 experimental configurations (3 solid lines) of a same structure. Displacement in log scale at a given observation point as a function of the frequency.

and yields the optimal prior pdf $p_{\mathbf{X}}^{\text{prior}}(\mathbf{x};\underline{\mathbf{x}}^{\text{opt}},\delta_X^{\text{opt}})$ for $\mathbf{X}$ and $p_{\mathbf{G}}^{\text{prior}}([G_M],[G_D],[G_K];\delta_G^{\text{opt}})$ for $[G_M]$, $[G_D]$, $[G_K]$.
(2) in identifying the posterior pdf $\mathbf{x} \mapsto p_{\mathbf{X}}^{\text{post}}(\mathbf{x})$ of the system-parameter uncertainties from the optimal prior pdf $p_{\mathbf{X}}^{\text{prior}}(\mathbf{x};\underline{\mathbf{x}}^{\text{opt}},\delta_X^{\text{opt}})$, in presence of the optimal prior pdf $p_{\mathbf{G}}^{\text{prior}}([G_M],[G_D],[G_K];\delta_G^{\text{opt}})$ of modeling errors, using the Bayes method and the experimental measurements.

The proposed identification procedure is based on the following considerations.
(1) In low-frequency band $\mathcal{B}_{\text{LF}}$, the frequency responses are driven by the eigenfrequencies which control the frequencies of the resonances and by the modal damping which controls the amplitudes of the resonances. In $\mathcal{B}_{\text{LF}}$, the role played by the modeling errors is small while the system-parameter uncertainties play a significant role. Consequently, the first eigenfrequencies are well adapted as the observations of the dynamical system in order to identify the optimal prior stochastic model and the posterior stochastic model of the system parameters which control the mass and the stiffness of the dynamical system.
(2) In medium-frequency band $\mathcal{B}_{\text{MF}}$, the frequency response functions are very sensitive to uncertainties and in particular, to model uncertainties. Consequently, the frequency response functions over $\mathcal{B}_{\text{MF}}$ are well adapted as observations of the dynamical system in order to identify the optimal prior stochastic model of model uncertainties induced by modeling errors.

Taking into account the above considerations, the different steps of the identification procedure will be the following:

- Step 1. Quantification of uncertainties induced by modeling errors in the medium-frequency range without system-parameter uncertainties. The parameter $\underline{\mathbf{x}}$ is then fixed to the nominal value. The dispersion parameter δ_X is then equal to zero. An optimal value δ_G^{opt} of δ_G is estimated using the maximum likelihood method for the observed stochastic frequency response functions over medium-frequency band $\mathcal{B}_{\text{MF}}$ and using the corresponding experimental frequency response functions.

- Step 2. Quantification of system-parameter uncertainties in the low-frequency range in presence of the model uncertainties quantified in Step 1.The parameter $\boldsymbol{\delta}_G$ is then fixed to the value $\boldsymbol{\delta}_G^{\text{opt}}$. The optimal values $\underline{\mathbf{x}}^{\text{opt}}$ and $\boldsymbol{\delta}_X^{\text{opt}}$ of the nominal value $\underline{\mathbf{x}}$ and the dispersion parameter $\boldsymbol{\delta}_X$ are then estimated using the maximum likelihood method for the observed first random eigenfrequencies in low-frequency band $\mathcal{B}_{\text{LF}}$ and using the corresponding experimental eigenfrequencies.

- Step 3. Identification of the posterior stochastic model of system-parameter uncertainties, in presence of the optimal stochastic model of model uncertainties induced by modeling errors, using the Bayesian method for the observed first random eigenfrequencies in low-frequency band $\mathcal{B}_{\text{LF}}$ and using the corresponding experimental first eigenfrequencies.

4.3. Frequency discretization

Let ν be the number of frequencies used for sampling the frequency interval $\mathcal{B}$. The corresponding frequency resolution (in rad/s) is $\Delta\omega = \omega_{\max}/\nu$ and the sampling frequency points are $\omega_k = k\,\Delta\omega$ for $k = 1, \ldots, \nu$.

(i) - Low-frequency band $\mathcal{B}_{\text{LF}} =]0\,, \omega_{\min}]$. Let $\omega_1, \ldots, \omega_{k_0}$ be all the sampling frequency points ω_k which belong to frequency band $\mathcal{B}_{\text{LF}}$ for $k = 1, \ldots, k_0$.

(ii) - Medium-frequency band $\mathcal{B}_{\text{MF}} =]\omega_{\min}\,, \omega_{\max}]$. Let $\omega_{k_1}, \ldots, \omega_\nu$ be all the sampling frequency points ω_k which belong to frequency band $\mathcal{B}_{\text{MF}}$ for $k = k_1, \ldots, \nu$. We then have $k_1 = k_0 + 1$ and $\omega_{k_0} \leq \omega_{\min} < \omega_{k_1}$.

4.4. Step 1 of the identification procedure

(i) - Observations for the identification of the prior stochastic model in medium-frequency band $\mathcal{B}_{\text{MF}}$. For identifying the stochastic models of model uncertainties induced by modeling errors, we will use as observations, the frequency response functions over the medium-frequency band $\mathcal{B}_{\text{MF}}$ at several points located on the structure, for which experimental measurements are available. We introduce the $\mathbb{C}^N$-valued observation $\mathbf{Z}(\omega) = (Z_1(\omega), \ldots, Z_N(\omega))$ of the stochastic computational model for which measurements are available. This observation is written as

$$\mathbf{Z}(\omega) = [H(\omega)]\,\mathbf{Y}(\omega)\,, \tag{28}$$

in which the observation operator $[H(\omega)]$ is a linear operator depending on ω. For instance, such a linear observation operator can be written as $[H(\omega)] = [h_1] + i\omega\,[h_2]$ in which $[h_1]$ and $[h_2]$ are two given $(N \times m)$ real matrices. In the time domain, the observation $\mathbf{Z}(t)$ is then written as $\mathbf{Z}(t) = [h_1]\,\mathbf{Y}(t) + [h_2]\,\dot{\mathbf{Y}}(t)$. For instance, if the N observed degrees of freedom are $Y_{j_1}, \ldots, Y_{j_N}$, then we introduce the $(N \times m)$ real matrix $[h_0]$ which extracts $Y_{j_1}, \ldots, Y_{j_N}$ from $\mathbf{Y}$. If the displacements are observed, then $[h_1] = [h_0]$ and $[h_2] = [0]$ while, if the velocities are observed, then $[h_1] = [0]$ and $[h_2] = [h_0]$. Clearly, observed displacements and velocities can be mixed in choosing adapted values of $[h_1]$ and $[h_2]$. If components of the strain tensor and/or the stress tensor are observed in a set of points of the structure, then $[h_1]$ can easily be constructed with the computational model and $[h_2] = [0]$. Measurement errors are due to measurement noise and/or to the lack of knowledge of the experimental configuration of the dynamical system for which measurements are done. The latter reason is the major source of measurement errors for complex dynamical systems. The real system built with a manufacturing process differs from the

design dynamical system and the real complex dynamical system is never completely known. In the low- and medium-frequency ranges (frequency band $\mathcal{B}$), the experimental FRF are usually estimated with the spectral analysis for stationary stochastic processes of the experimental data, in presence of extraneous input and output noise. This type of estimation, based on the use of the cross-spectral density functions of the input and the output stationary stochastic processes, allows the effects of the extraneous noises to be removed and consequently, the experimental FRF which are estimated in presence of measurement errors, do not depend of these noises [13, 14]. Consequently, it is assumed that the experimental FRF are not affected by measurement noise. For any realization $\theta'_{\ell'}$, with $\ell' = 1, \ldots, \nu_{\rm NP}$, and for $k = k_1, \ldots, \nu$, the realization of complex random vector $\mathbf{Z}(\omega_k)$ is written as

$$\mathbf{z}_{\ell'}(\omega_k) = \mathbf{Z}(\theta'_{\ell'}; \omega_k) = [H(\omega_k)]\, \mathbf{y}_{\ell'}(\omega_k)\,, \tag{29}$$

in which $\mathbf{y}_{\ell'}(\omega_k)$ is computed using Eqs. (24) and (25) (for $\mathbf{X} = \underline{\mathbf{x}}$, $\boldsymbol{\delta}_X = 0$ and fixed $\boldsymbol{\delta}_G$). Let $N_{\rm obs}$ be defined by $N_{\rm obs} = N \times (\nu - k_1 + 1)$ such that $n < N_{\rm obs} < \nu_{\rm p} \times \nu_{\rm NP}$. For $j = 1, \ldots, N$ and $k = k_1, \ldots, \nu$, let $r = 1, \ldots, N_{\rm obs}$ be the index associated with j and k. Let $\mathbf{V} = (V_1, \ldots, V_{N_{\rm obs}})$ be the random vector such that

$$V_r = \log_{10} |Z_j(\omega_k)|\,, \tag{30}$$

whose realization

$$\mathbf{v}_{\ell'} = \mathbf{V}(\theta'_{\ell'}) \tag{31}$$

is such that,

$$\{\mathbf{v}_{\ell'}\}_r = \log_{10} |\{\mathbf{z}_{\ell'}(\omega_k)\}_j|\,. \tag{32}$$

Finally, we introduce the observation vector $\mathbf{W} = (W_1, \ldots, W_n)$, with values in $\mathbb{R}^n$, which will be used for the identification of the stochastic models of uncertainties. This observation vector corresponds to a statistical reduction of order n (the dimension of the reduced-order mean computational model) of the random vector $\mathbf{V}$, using the principal component analysis for $\mathbf{V}$. It should be noted that the order n of such a statistical reduction could be increased, but this choice corresponds to a good compromise for constructing the observation vector in the context of the identification procedure. In addition, vector $\mathbf{W}$ is introduced as an observation for identifying the stochastic models of uncertainties. Therefore, we do not seek to build an observation that is strictly equivalent to $\mathbf{V}$, which means that we choose, *a priori*, the value n, and it is no necessary that the convergence of $\mathbf{W}$ towards $\mathbf{V}$ be reached, *i.e*, to have an equivalence of $\mathbf{W}$ with $\mathbf{V}$. This means that n is chosen in order that the probability distribution of $\mathbf{W}$ be sufficiently sensitive to small variations of parameters $\boldsymbol{\delta}_G$ of the prior stochastic model of model uncertainties that we will have to identify. Let $\mathbf{m}_{\mathbf{V}} = E\{\mathbf{V}\}$ be the mean value of $\mathbf{V}$ and let $[C_{\mathbf{V}}] = [R_{\mathbf{V}}] - \mathbf{m}_{\mathbf{V}}\, \mathbf{m}_{\mathbf{V}}^T$ be its covariance matrix in which $[R_{\mathbf{V}}] = E\{\mathbf{V}\, \mathbf{V}^T\}$. We have the estimations,

$$\mathbf{m}_{\mathbf{V}} \simeq \frac{1}{\nu_{\rm NP}} \sum_{\ell'=1}^{\nu_{\rm NP}} \mathbf{v}_{\ell'}\ ,\ [R_{\mathbf{V}}] \simeq \frac{1}{\nu_{\rm NP}} \sum_{\ell'=1}^{\nu_{\rm NP}} \mathbf{v}_{\ell'} \mathbf{v}_{\ell'}^T\,. \tag{33}$$

Let $[C_{\mathbf{V}}]\, \boldsymbol{\psi} = \eta\, \boldsymbol{\psi}$ be the eigenvalue problem for which the n first largest eigenvalues are denoted by $\eta_1 \geq \eta_2 \geq \ldots \geq \eta_n$ and for which the associated eigenvectors $\{\boldsymbol{\psi}_1, \boldsymbol{\psi}_2, \ldots, \boldsymbol{\psi}_n\}$ are such that $< \boldsymbol{\psi}_\alpha\, , \boldsymbol{\psi}_\beta > = \delta_{\alpha\beta}$. Consequently, for all α in $\{1, \ldots, n\}$, the component W_α of observation vector $\mathbf{W}$ is written as

$$W_\alpha = \frac{1}{\sqrt{\eta_\alpha}} < \mathbf{V} - \mathbf{m}_{\mathbf{V}}\, , \boldsymbol{\psi}_\alpha > \ . \tag{34}$$

We have $E\{\mathbf{W}\} = 0$ and $E\{\mathbf{W}\,\mathbf{W}^T\} = [\,I_n]$. For $\ell' = 1, \ldots, \nu_{\rm NP}$, the realization

$$\mathbf{w}_{\ell'} = \mathbf{W}(\theta'_{\ell'}) \tag{35}$$

is such that, for $\alpha = 1, \ldots, n$,

$$\{\mathbf{w}_{\ell'}\}_\alpha = \frac{1}{\sqrt{\eta_\alpha}} < \mathbf{v}_{\ell'} - \mathbf{m}_\mathbf{V}\,, \boldsymbol{\psi}_\alpha > \ . \tag{36}$$

(ii) - Experimental measurements. For frequency sampling ω_k with $k = k_1, \ldots, \nu$, it is assumed that $\nu_{\rm exp}$ experimental measurements $\mathbf{z}^{1,\rm exp}(\omega_k), \ldots, \mathbf{z}^{\nu_{\rm exp},\rm exp}(\omega_k)$ are available for the observation $\mathbf{Z}$. Taking into account Eq. (32), for each $s = 1, \ldots, \nu_{\rm exp}$, the vector $\mathbf{v}^{s,\rm exp} = (v_1^{s,\rm exp}, \ldots, v_{N_{\rm obs}}^{s,\rm exp})$ is introduced such that

$$v_r^{s,\rm exp} = \log_{10} |z_j^{\,s,\rm exp}(\omega_k)|\,. \tag{37}$$

in which $r = 1, \ldots, N_{\rm obs}$ is the index associated with j and k. Taking into account Eq. (36), let $\mathbf{w}^{s,\rm exp} = (w_1^{s,\rm exp}, \ldots, w_n^{s,\rm exp})$ be the vector of the experimental observation such that, for $\alpha = 1, \ldots, n$,

$$w_\alpha^{s,\rm exp} = \frac{1}{\sqrt{\eta_\alpha}} < \mathbf{v}^{s,\rm exp} - \mathbf{m}_\mathbf{V}\,, \boldsymbol{\psi}_\alpha > \ . \tag{38}$$

It should be noted that the projected experimental observation $\mathbf{w}^{\,s,\rm exp} = \mathbf{w}^{s,\rm exp}(\boldsymbol{\delta}_G)$ depends on the parameters $\boldsymbol{\delta}_G$ of the prior stochastic model of model uncertainties, due to the presence of η_α, $\boldsymbol{\psi}_\alpha$ and $\mathbf{m}_\mathbf{V}$ in Eq. (38).

(iii) - Estimation of the optimal value $\boldsymbol{\delta}_G^{\rm opt}$ of $\boldsymbol{\delta}_G$. The optimal value $\boldsymbol{\delta}_G^{\rm opt}$ of $\boldsymbol{\delta}_G$ is estimated by maximizing the logarithm of the likelihood function,

$$\boldsymbol{\delta}_G^{\rm opt} = \arg\max_{\boldsymbol{\delta}_G \in C_G} \{ \sum_{s=1}^{\nu_{\rm exp}} \log\ p_\mathbf{W}(\mathbf{w}^{s,\rm exp}(\boldsymbol{\delta}_G); \boldsymbol{\delta}_G) \}\,. \tag{39}$$

in which $p_\mathbf{W}(\mathbf{w}^{s,\rm exp}(\boldsymbol{\delta}_G); \boldsymbol{\delta}_G)$ is the value of the pdf $\mathbf{w} \mapsto p_\mathbf{W}(\mathbf{w}; \boldsymbol{\delta}_G)$ of the random vector $\mathbf{W}$ for $\mathbf{w} = \mathbf{w}^{s,\rm exp}(\boldsymbol{\delta}_G)$, which is estimated for each value $\mathbf{w}^{s,\rm exp}(\boldsymbol{\delta}_G)$ of $\mathbf{w}$ by nonparametric statistics in using the multivariate Gaussian kernel density estimation method with the $\nu_{\rm NP}$ independent realizations $\mathbf{w}_1, \ldots, \mathbf{w}_{\nu_{\rm NP}}$. The optimization problem defined by Eq. (39) is not convex and must be solved using random search or genetic algorithms. An initial value $\boldsymbol{\delta}_G^{\,0}$ can be computed using a Gaussian approximation, $p_\mathbf{W}^g$, of $p_\mathbf{W}$. This initial value can be used as an approximation of the optimal value or can be used as the center of the region of C_G, in which the optimal value is searched. From Eq. (39), it can be deduced that

$$\boldsymbol{\delta}_G^0 = \arg\max_{\boldsymbol{\delta}_G \in C_G} J_g(\boldsymbol{\delta}_G)\,, \tag{40}$$

$$J_g(\boldsymbol{\delta}_G) = \sum_{s=1}^{\nu_{\rm exp}} \log\ p_\mathbf{W}^g(\mathbf{w}^{s,\rm exp}(\boldsymbol{\delta}_G); \boldsymbol{\delta}_G)\,, \tag{41}$$

where the cost function J_g is written as

$$\begin{aligned} J_g(\boldsymbol{\delta}_G) = &-\frac{1}{2\ln(10)} \{ \nu_{\rm exp}\, n \ln(2\pi) \\ &+ \sum_{s=1}^{\nu_{\rm exp}} \|\mathbf{w}^{s,\rm exp}(\boldsymbol{\delta}_G)\|^2 \}\,, \end{aligned} \tag{42}$$

where $\mathbf{w}^{s,\rm exp}(\boldsymbol{\delta}_G)$ is computed using Eq. (38).

4.5. Step 2 of the identification procedure

(i) - Observations for the identification of the prior stochastic model in low-frequency band $\mathcal{B}_{\mathrm{LF}}$. For identifying the stochastic model of system-parameter uncertainties, we will use as observations, the first N_{eig} random eigenfrequencies belonging to low-frequency band $\mathcal{B}_{\mathrm{LF}}$, for which experimental measurements are available. We then introduce the random vector $\mathbf{\Omega} = (\Omega_1, \ldots, \Omega_{N_{\mathrm{eig}}})$ of the first N_{eig} random eigenfrequencies $0 < \Omega_1 \leq \ldots \leq \Omega_{N_{\mathrm{eig}}}$ whose realizations $\Omega_1(\theta_\ell, \theta'_{\ell'}) \leq \ldots \leq \Omega_{N_{\mathrm{eig}}}(\theta_\ell, \theta'_{\ell'})$ are computed using Eq. (19) for given $\underline{\mathbf{x}}$, $\boldsymbol{\delta}_X$ and for $\boldsymbol{\delta}_G = \boldsymbol{\delta}_G^{\mathrm{opt}}$ estimated in Step 1. For any realization $(\theta_\ell, \theta'_{\ell'})$, with $\ell = 1, \ldots, \nu_{\mathrm{P}}$ and $\ell' = 1, \ldots, \nu_{\mathrm{NP}}$, the realization of random vector $\mathbf{\Omega}$ is written as

$$\boldsymbol{\omega}_{\ell,\ell'} = \mathbf{\Omega}(\theta_\ell, \theta'_{\ell'}) = (\Omega_1(\theta_\ell, \theta'_{\ell'}), \ldots, \Omega_{N_{\mathrm{eig}}}(\theta_\ell, \theta'_{\ell'})). \tag{43}$$

(ii) - Experimental measurements. The first experimental eigenfrequencies are usually deduced from the experimental frequency response functions and consequently, are not affected by measurement noise (see Section 4.4-(i)). Therefore, ν_{exp} experimental measurements of the first eigenfrequencies are available. For each experimental configuration s with $s = 1, \ldots, \nu_{\mathrm{exp}}$, let $\boldsymbol{\omega}^{s,\mathrm{exp}} = (\omega^{s,\mathrm{exp}}_{\alpha_1}, \ldots, \omega^{s,\mathrm{exp}}_{\alpha_{N_{\mathrm{eig}}}})$ be the vector of the N_{eig} experimental eigenfrequencies associated with the first N_{eig} random eigenfrequencies $\Omega_1, \ldots, \Omega_{N_{\mathrm{eig}}}$.

(iii) - Estimation of the optimal values $(\underline{\mathbf{x}}^{\mathrm{opt}}, \boldsymbol{\delta}_X^{\mathrm{opt}})$ *of* $(\underline{\mathbf{x}}, \boldsymbol{\delta}_X)$. It is recalled that $\boldsymbol{\delta}_G = \boldsymbol{\delta}_G^{\mathrm{opt}}$. The optimal value $(\underline{\mathbf{x}}^{\mathrm{opt}}, \boldsymbol{\delta}_X^{\mathrm{opt}})$ of $(\underline{\mathbf{x}}, \boldsymbol{\delta}_X)$ is estimated by maximizing the logarithm of the likelihood function,

$$\begin{aligned}(\underline{\mathbf{x}}^{\mathrm{opt}}, \boldsymbol{\delta}_X^{\mathrm{opt}}) = \arg \max_{(\underline{\mathbf{x}}, \boldsymbol{\delta}_X) \in C_{\mathrm{par}} \times C_X} \\ \{\sum_{s=1}^{\nu_{\mathrm{exp}}} \log\, p_{\mathbf{\Omega}}(\boldsymbol{\omega}^{s,\mathrm{exp}}; \underline{\mathbf{x}}, \boldsymbol{\delta}_X, \boldsymbol{\delta}_G^{\mathrm{opt}})\},\end{aligned} \tag{44}$$

in which $p_{\mathbf{\Omega}}(\boldsymbol{\omega}^{s,\mathrm{exp}}; \underline{\mathbf{x}}, \boldsymbol{\delta}_X, \boldsymbol{\delta}_G^{\mathrm{opt}})$ is the value, for $\boldsymbol{\omega} = \boldsymbol{\omega}^{s,\mathrm{exp}}$, of the pdf $\boldsymbol{\omega} \mapsto p_{\mathbf{\Omega}}(\boldsymbol{\omega}; \underline{\mathbf{x}}, \boldsymbol{\delta}_X, \boldsymbol{\delta}_G^{\mathrm{opt}})$ of the random vector $\mathbf{\Omega}$. Since N_{eig} is small (a few units), the multivariate Gaussian kernel density estimation method is directly used without difficulties for estimating $p_{\mathbf{\Omega}}(\boldsymbol{\omega}^{s,\mathrm{exp}}; \underline{\mathbf{x}}, \boldsymbol{\delta}_X, \boldsymbol{\delta}_G^{\mathrm{opt}})$ for each value $\boldsymbol{\omega}^{s,\mathrm{exp}}$ of $\boldsymbol{\omega}$ using the $\nu_{\mathrm{P}}\nu_{\mathrm{NP}}$ independent realizations $\boldsymbol{\omega}_{\ell,\ell'}$.

4.6. Step 3 of the identification procedure

This step is devoted to the identification of the posterior stochastic model of system-parameter uncertainties using the Bayesian method and in presence of model uncertainties. For $\ell = 1, \ldots, \nu_{\mathrm{P}}$ and $\ell' = 1, \ldots, \nu_{\mathrm{NP}}$, let $\boldsymbol{\omega}_{\ell,\ell'}$ be the realizations of random vector $\mathbf{\Omega}$, computed with Eq. (19) for the optimal value $(\underline{\mathbf{x}}^{\mathrm{opt}}, \boldsymbol{\delta}_X^{\mathrm{opt}}, \boldsymbol{\delta}_G^{\mathrm{opt}})$ of the parameter $(\underline{\mathbf{x}}, \boldsymbol{\delta}_X, \boldsymbol{\delta}_G)$ of the prior stochastic models of uncertainties. Let be $p^{\mathrm{prior}}_{\mathbf{X}}(\mathbf{x}) = p^{\mathrm{prior}}_{\mathbf{X}}(\mathbf{x}; \underline{\mathbf{x}}^{\mathrm{opt}}, \boldsymbol{\delta}_X^{\mathrm{opt}})$. The Bayesian method allows the posterior pdf, $p^{\mathrm{post}}_{\mathbf{X}}(\mathbf{x})$, to be calculated by

$$p^{\mathrm{post}}_{\mathbf{X}}(\mathbf{x}) = \mathcal{L}(\mathbf{x})\, p^{\mathrm{prior}}_{\mathbf{X}}(\mathbf{x}), \tag{45}$$

in which $\mathbf{x} \mapsto \mathcal{L}(\mathbf{x})$ is the normalized likelihood function defined on $\mathbb{R}^{n_p}$, with positive values, such that

$$\mathcal{L}(\mathbf{x}) = \frac{\prod_{s=1}^{\nu_{\mathrm{exp}}} p_{\mathbf{\Omega}|\mathbf{X}}(\boldsymbol{\omega}^{s,\mathrm{exp}}|\mathbf{x})}{E\{\prod_{s=1}^{\nu_{\mathrm{exp}}} p_{\mathbf{\Omega}|\mathbf{X}}(\boldsymbol{\omega}^{s,\mathrm{exp}}|\mathbf{X})\}}. \tag{46}$$

In Eq. (46), $p_{\mathbf{\Omega}|\mathbf{X}}(\boldsymbol{\omega}^{s,\exp}|\mathbf{x})$ is the experimental value (see Section 4.5-(ii)) of the conditional probability density function $\boldsymbol{\omega} \mapsto p_{\mathbf{\Omega}|\mathbf{X}}(\boldsymbol{\omega}|\mathbf{x})$ of the random eigenfrequencies $\mathbf{\Omega}|\mathbf{X}$ given $\mathbf{X} = \mathbf{x}$ in C_{par}. Equation (46) shows that normalized likelihood function $\mathcal{L}$ must verify the following equation,

$$E\{\mathcal{L}(\mathbf{X})\} = \int_{\mathbb{R}^{n_p}} \mathcal{L}(\mathbf{x})\, p_{\mathbf{X}}^{\text{prior}}(\mathbf{x})\, d\mathbf{x} = 1\,. \tag{47}$$

Similarly to Section 4.5, for all fixed ℓ and for each value $\boldsymbol{\omega}^{s,\exp}$ of $\boldsymbol{\omega}$, the value $p_{\mathbf{\Omega}|\mathbf{X}}(\boldsymbol{\omega}^{s,\exp}|\mathbf{X}(\theta_\ell))$ of the conditional pdf $\boldsymbol{\omega} \mapsto p_{\mathbf{\Omega}|\mathbf{X}}(\boldsymbol{\omega}|\mathbf{X}(\theta_\ell))$ is estimated by nonparametric statistics using the multivariate Gaussian kernel density estimation method with the ν_{NP} independent realizations $\boldsymbol{\omega}_{\ell,1}, \ldots, \boldsymbol{\omega}_{\ell,\nu_{\text{NP}}}$. From Eq. (46), it can be deduced that

$$\mathcal{L}(\mathbf{X}(\theta_\ell)) \simeq \frac{\prod_{s=1}^{\nu_{\exp}} p_{\mathbf{\Omega}|\mathbf{X}}(\boldsymbol{\omega}^{s,\exp}|\mathbf{X}(\theta_\ell))}{\frac{1}{\nu_{\text{P}}}\sum_{l=1}^{\nu_{\text{P}}} \prod_{s=1}^{\nu_{\exp}} p_{\mathbf{\Omega}|\mathbf{X}}(\boldsymbol{\omega}^{s,\exp}|\mathbf{X}(\theta_l))}\,. \tag{48}$$

The posterior pdf of $\mathbf{X}$ is given by Eq. (45) and can be rewritten as

$$\begin{aligned} p_{\mathbf{X}}^{\text{post}}(\mathbf{x}) &= \textstyle\int_{\mathbb{R}^{n_p}} \mathcal{L}(\mathbf{y})\, p_{\mathbf{X}}^{\text{prior}}(\mathbf{y})\, \delta_0(\mathbf{y}-\mathbf{x})\, d\mathbf{y} \\ &= E\{\delta_0(\mathbf{X}-\mathbf{x})\, \mathcal{L}(\mathbf{X})\}\,, \end{aligned} \tag{49}$$

in which $\delta_0(\mathbf{y}-\mathbf{x})\, d\mathbf{y}$ is the Dirac measure on $\mathbb{R}^{n_p}$ at point $\mathbf{x}$, and where $\mathbf{X}$ is always the random variable for which the probability distribution is defined by the prior stochastic model. For fixed $\mathbf{x} = (x_1, \ldots, x_{n_p})$, if the multivariate Gaussian kernel density estimation method is used, we obtain

$$\begin{aligned} &p_{\mathbf{X}}^{\text{post}}(\mathbf{x}) \simeq \frac{1}{\nu_{\text{P}}} \times \\ &\sum_{\ell=1}^{\nu_{\text{P}}} \mathcal{L}(\mathbf{X}(\theta_\ell)) \prod_{j=1}^{n_p} \left\{ \frac{1}{h_j}\, \mathbb{k}\left(\frac{X_j(\theta_\ell) - x_j}{h_j} \right) \right\}, \end{aligned} \tag{50}$$

in which $\mathcal{L}(\mathbf{X}(\theta_\ell))$ is given by Eq. (48), where $\mathbb{k}(w) = (2\pi)^{-1/2} \exp(-w^2/2)$ and where h_j is defined [16] by

$$h_j = \sigma_j \left\{ \frac{4}{\nu_{\text{P}}(2+n_p)} \right\}^{1/(4+n_p)}, \tag{51}$$

in which $\sigma_j = \sqrt{R_j - m_j^2}$ with

$$m_j \simeq \frac{1}{\nu_{\text{P}}} \sum_{\ell=1}^{\nu_{\text{P}}} X_j(\theta_\ell)\ ,\ R_j \simeq \frac{1}{\nu_{\text{P}}} \sum_{\ell=1}^{\nu_{\text{P}}} X_j(\theta_\ell)^2. \tag{52}$$

From Eq. (50), it can be deduced the posterior marginal pdf of X_j which is then given by

$$p_{X_j}^{\text{post}}(x_j) \simeq \frac{1}{\nu_{\text{P}}} \sum_{\ell=1}^{\nu_{\text{P}}} \mathcal{L}(\mathbf{X}(\theta_\ell)) \frac{1}{h_j}\, \mathbb{k}\left(\frac{X_j(\theta_\ell) - x_j}{h_j} \right). \tag{53}$$

5. Posterior stochastic model of the responses and quality assessment

In this section, it is shown how the confidence regions of the frequency response functions are computed with the stochastic reduced-order computational model for which the posterior stochastic model of system-parameter uncertainties and the optimal prior stochastic model of model uncertainties are used (see Section 4). The stochastic response functions are computed over the low- and medium-frequency band $\mathcal{B} = \mathcal{B}_{\text{LF}} \cup \mathcal{B}_{\text{MF}}$. The observations introduced in this section are observations used in the identification procedure and other observations which have not been used in the identification of the stochastic model. The comparisons of experimental frequency response functions (not used for the identification) with the corresponding computed random frequency response functions are usually called the quality assessment.

5.1. Observations of the dynamical system for the quality assessment

Let $\mathbf{Z}^{\text{obs}}(\omega) = (Z_1^{\text{obs}}(\omega), \ldots, Z_{N_{\text{obs}}}^{\text{obs}}(\omega))$ be the observation vector of the stochastic reduced-order computational model such that

$$\mathbf{Z}^{\text{obs}}(\omega) = [H^{\text{obs}}(\omega)]\, \mathbf{Y}(\omega)\,, \tag{54}$$

in which $[H^{\text{obs}}(\omega)]$ is the observation operator which will be, for instance, written as $[H^{\text{obs}}(\omega)] = [h_1^{\text{obs}}] + i\omega\,[h_2^{\text{obs}}]$ in which $[h_1^{\text{obs}}]$ and $[h_2^{\text{obs}}]$ are two given $(N_{\text{obs}} \times m)$ real matrices. Let $\{\omega_k, k = 1, \ldots, \nu\}$ be the sampling frequency points of frequency band $\mathcal{B}$, introduced in Section 4.3. For $\ell = 1, \ldots, \nu_{\text{P}}$ and $\ell' = 1, \ldots, \nu_{\text{NP}}$, the realization $\mathbf{z}_{\ell,\ell'}^{\text{obs}}(\omega_k) = \mathbf{Z}^{\text{obs}}(\theta_\ell, \theta'_{\ell'}; \omega_k)$ is given by

$$\mathbf{z}_{\ell,\ell'}^{\text{obs}}(\omega_k) = [H^{\text{obs}}(\omega_k)]\, \mathbf{y}_{\ell,\ell'}(\omega_k)\,, \tag{55}$$

in which $\mathbf{y}_{\ell,\ell'}(\omega_k)$ is computed with Eqs. (21) and (22) for which the optimal prior stochastic models $p_{\mathbf{X}}^{\text{prior}}(\mathbf{x}; \underline{\mathbf{x}}^{\text{opt}}, \boldsymbol{\delta}_X^{\text{opt}})$ and $p_{\mathbf{G}}^{\text{prior}}([G_M],[G_D],[G_K];\boldsymbol{\delta}_G^{\text{opt}})$ of uncertainties are used. Below, j is fixed in $\{1, \ldots, N_{\text{obs}}\}$. In order to simplify the notation, j is removed in the quantities depending on j. Let $U(\omega_k)$ be the real-valued random observation such that $U(\omega_k) = \log_{10} |Z_j^{\text{obs}}(\omega_k)|$. The realization $u_{\ell,\ell'}(\omega_k) = U(\theta_\ell, \theta'_{\ell'}; \omega_k)$ of random variable $U(\omega_k)$ is such that

$$u_{\ell,\ell'}(\omega_k) = \log_{10} |\{\mathbf{z}_{\ell,\ell'}^{\text{obs}}(\omega_k)\}_j|\,. \tag{56}$$

5.2. Posterior probability density function of an observation

The posterior probability density function $u \mapsto p_{U(\omega_k)}^{\text{post}}(u)$ of the real-valued random observation $U(\omega_k)$ is given by

$$p_{U(\omega_k)}^{\text{post}}(u) = \int_{\mathbb{R}^{n_p}} p_{U(\omega_k)|\mathbf{X}}(u|\mathbf{x})\, p_{\mathbf{X}}^{\text{post}}(\mathbf{x})\, d\mathbf{x}\,, \tag{57}$$

in which $p_{U(\omega_k)|\mathbf{X}}(u|\mathbf{x})$ is the conditional pdf of $U(\omega_k)$, given $\mathbf{X} = \mathbf{x}$. From Eq. (45), it can be deduced that

$$\begin{aligned} p_{U(\omega_k)}^{\text{post}}(u) &= \int_{\mathbb{R}^{n_p}} p_{U(\omega_k)|\mathbf{X}}(u|\mathbf{x})\, \mathcal{L}(\mathbf{x})\, p_{\mathbf{X}}^{\text{prior}}(\mathbf{x})\, d\mathbf{x} \\ &= E\{\mathcal{L}(\mathbf{X}^{\text{prior}})\, p_{U(\omega_k)|\mathbf{X}}(u|\mathbf{X}^{\text{prior}})\}\,, \end{aligned} \tag{58}$$

in which $\mathbf{X}^{\text{prior}}$ denotes the random variable $\mathbf{X}$ for which the probability distribution is defined by the optimal prior pdf $p_{\mathbf{X}}^{\text{prior}}(\mathbf{x}; \underline{\mathbf{x}}^{\text{opt}}, \boldsymbol{\delta}_X^{\text{opt}})$. The following estimation of Eq. (58) can be used,

$$p_{U(\omega_k)}^{\text{post}}(u) \simeq \frac{1}{\nu_{\text{P}}} \sum_{\ell=1}^{\nu_{\text{P}}} \mathcal{L}(\mathbf{X}(\theta_\ell))\, p_{U(\omega_k)|\mathbf{X}}(u|\mathbf{X}(\theta_\ell)), \tag{59}$$

in which $\mathcal{L}(\mathbf{X}(\theta_\ell))$ is given by Eq. (48). The conditional pdf $p_{U(\omega_k)|\mathbf{X}}(u|\mathbf{X}(\theta_\ell))$ can be estimated by using the Gaussian kernel density method,

$$p_{U(\omega_k)|\mathbf{X}}(u|\mathbf{X}(\theta_\ell)) \simeq \frac{1}{\nu_{\text{NP}}} \sum_{\ell'=1}^{\nu_{\text{NP}}} \frac{1}{h_\ell(\omega_k)} \mathbb{k}\left(\frac{u_{\ell,\ell'}(\omega_k) - u}{h_\ell(\omega_k)}\right) \tag{60}$$

in which $u_{\ell,\ell'}(\omega_k)$ is given by Eq. (56) and where the constant $h_\ell(\omega_k)$ is written [16] as

$$h_\ell(\omega_k) = \sigma_\ell(\omega_k) \left\{\frac{4}{3\,\nu_{\text{NP}}}\right\}^{1/5}, \tag{61}$$

in which $\sigma_\ell(\omega_k) = \sqrt{R_\ell(\omega_k) - m_\ell(\omega_k)^2}$ with

$$\begin{aligned} m_\ell(\omega_k) &\simeq \frac{1}{\nu_{\text{NP}}} \sum_{\ell'=1}^{\nu_{\text{NP}}} u_{\ell,\ell'}(\omega_k)\,, \\ R_\ell(\omega_k) &\simeq \frac{1}{\nu_{\text{NP}}} \sum_{\ell'=1}^{\nu_{\text{NP}}} u_{\ell,\ell'}(\omega_k)^2\,. \end{aligned} \tag{62}$$

5.3. Posterior confidence region of the observation in the frequency domain

For a probability level P_c, let $\{u^+(\omega_k), k = 1, \ldots, \nu\}$ and $\{u^-(\omega_k), k = 1, \ldots, \nu\}$ be the upper and the lower envelopes of the confidence region of the random sampled frequency response $\{U(\omega_k), k = 1, \ldots, \nu\}$, such that, for $k = 1, \ldots, \nu$,

$$\text{Proba}\{u^-(\omega_k) < U(\omega_k) \leq u^+(\omega_k)\} = P_c\,. \tag{63}$$

Consequently, for $k = 1, \ldots, \nu$, the upper and lower envelopes are defined, by

$$\begin{aligned} u^+(\omega_k) &= \zeta(\frac{1 + P_c}{2}; \omega_k)\,, \\ u^-(\omega_k) &= \zeta(\frac{1 - P_c}{2}; \omega_k)\,. \end{aligned} \tag{64}$$

The p-th quantile is defined by

$$\zeta(p; \omega_k) = \inf\{u : F_{U(\omega_k)}^{\text{post}}(u) \geq p\}\,. \tag{65}$$

The cumulative distribution function $F_{U(\omega_k)}^{\text{post}}$ of random variable $U(\omega_k)$ is defined by

$$\begin{aligned} F_{U(\omega_k)}^{\text{post}}(u) &= \text{Proba}\{U(\omega_k) \leq u\} \\ &= \textstyle\int_{-\infty}^{u} p_{U(\omega_k)}^{\text{post}}(v; \omega_k)\, dv\,. \end{aligned} \tag{66}$$

From Eqs. (59) and (66), it can be deduced that

$$F^{\text{post}}_{U(\omega_k)}(u) \simeq \frac{1}{\nu_{\text{P}}} \sum_{\ell=1}^{\nu_{\text{P}}} \mathcal{L}(\mathbf{X}(\theta_\ell))\, F_{U(\omega_k)|\mathbf{X}}(u|\mathbf{X}(\theta_\ell)), \tag{67}$$

in which the conditional cumulative distribution function, $F_{U(\omega_k)|\mathbf{X}}(u|\mathbf{X}(\theta_\ell)) = \int_{-\infty}^{u} p_{U(\omega_k)|\mathbf{X}}(v|\mathbf{X}(\theta_\ell))\, dv$, is estimated using the Gaussian kernel density method and can be written, taking into account Eq. (60), as

$$F_{U(\omega_k)|\mathbf{X}}(u|\mathbf{X}(\theta_\ell)) \simeq \frac{1}{\nu_{\text{NP}}} \sum_{\ell'=1}^{\nu_{\text{NP}}} F_{\mathbb{k}}\left(\frac{u - u_{\ell,\ell'}(\omega_k)}{h_\ell(\omega_k)}\right), \tag{68}$$

in which $h_\ell(\omega_k)$ is defined by Eq. (61) and where $F_{\mathbb{k}}(u) = \int_{-\infty}^{u} \mathbb{k}(v)\, dv$.

6. Application

In this section, a validation of the previous theory is presented for which the real system corresponds to a three-dimensional slender damped elastic bounded medium for which the mean computational model is constructed using the Timoshenko beam theory. The question is not to discuss the choice of the Timoshenko beam theory to construct the mean computational model but to analyze how the system-parameter uncertainties and the model uncertainties induced by modeling errors can be quantified using simulated experiments of the real system and how the predictions performed with the mean computational model can be improved in taking into account uncertainties.

6.1. Designed system

The designed system is a slender cylindrical elastic medium defined in a cartesian co-ordinate system $Ox_1x_2x_3$ (see Fig. 2). The cylinder has length $L_1 = 0.01$ m and has a rectangular section with height $L_2 = 0.001$ m and width $L_3 = 0.002$ m. The two end sections are located at $x_1 = 0$ and $x_1 = 0.01$. The origin O is in the corner of the end section and Ox_1 is parallel to the cylinder axis. The axis Ox_2 is the transversal axis along the height and Ox_3 is the lateral axis along the width. The neutral line has for equation $\{0 \leq x_1 \leq 0.01\,;\, x_2 = 0.0005\,;\, x_3 = 0.001\}$. The elastic medium is made of a homogeneous and isotropic elastic material for which the Young modulus is 10^{10} N/m^2, the Poisson coefficient is 0.15 and the mass density is $1,500$ Kg/m^3. A damping term is added and is described by a critical damping rate of 0.01 for each elastic mode used in the reduced-order model. Concerning the boundary conditions, the displacements are locked on the two lines defined by $\{(x_1, x_2, x_3) : x_1 = 0\,; x_2 = 0.0005\,;\, 0 \leq x_3 \leq 0.002\}$ and by $\{(x_1, x_2, x_3) : x_1 = 0.01\,; x_2 = 0.0005\,;\, 0 \leq x_3 \leq 0.002\}$. The frequency band of analysis is $\mathcal{B} = 2\pi\times]0\,, 1.2 \times 10^6]$ rad/s. The external load is a point load applied to the point $(x_1 = 0.0042, x_2 = 0.001, x_3 = 0.001)$ and its Fourier transform is the vector-valued function $\omega \mapsto (0, -\mathbb{1}_{\mathcal{B}}(\omega), 0)$ in which $\mathbb{1}_{\mathcal{B}}(\omega) = 1$ if frequency ω belongs to $\mathcal{B}$ and $\mathbb{1}_{\mathcal{B}}(\omega) = 0$ if ω does not belong to $\mathcal{B}$. We are interested in the transversal displacement along Ox_2 in the plane Ox_1x_2 of the neutral line. For Step 1 of the identification procedure, the following six observation points P_1, P_2, P_3, P_4, P_5 and P_6 are considered in the neutral line for which x_1 are 0.0013, 0.0029, 0.0042, 0.005, 0.0064 and 0.0084 m respectively. For the quality assessment, the following four observation points QA_1, QA_2, QA_3 and QA_4 are considered in the neutral line for which x_1 are 0.0021, 0.0035, 0.0057 and 0.0074 m respectively.

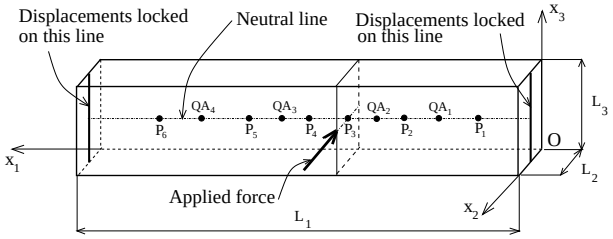

Figure 2: Scheme of the designed mechanical system.

6.2. Simulated experiments of the real system

In this application, $\nu_{\exp} = 5$ simulated experiments of the real system are used to perform the identification of the stochastic models of uncertainties. The design system described in Section 6.1 is used with a homogeneous and isotropic elastic material for which the Young modulus is 10^{10} N/m^2, the Poisson coefficient is 0.15 and the mass density is $1,500$ Kg/m^3. A 3D computational model of the design system is constructed with a finite element mesh made up of $100 \times 10 \times 20 = 20,000$ three-dimensional 8-nodes solid elements. There are $23,331$ nodes and a total of $69,867$ degrees of freedom (due to the boundary conditions, the displacement is zero for 2×21 nodes). There are 165 eigenfrequencies in frequency band $\mathcal{B}$. The fundamental eigenfrequency is $11,936$ Hz. The five simulated experiments of the real system are then constructed as five realizations of the random computational model corresponding to the 3D computational model of the design system for which random parameters have been introduced. The Young modulus, the Poisson coefficient and the mass density are modeled as three independent random variables with values in $\mathbb{R}^+$. The Poisson coefficient has a bounded support included in $]-1, 0.5[$. The Young modulus and the mass density are random variables with positive values. The mean values of these three random variables are equal to the values of the designed system. The coefficients of variation of each random variable is 0.1. The random Young modulus is written as the product of two independent Gamma random variables and the random Poisson coefficient as the product of two independent uniform random variables. With respect to the nominal computational model, the uncertain model parameters will be induced by the stochastic computational model used for simulating the experiments and the model uncertainties are mainly due to the modeling errors induced by the use of a Timoshenko beam for modeling a 3D slender elastic body. Each realization of the frequency response functions are calculated using modal analysis with the first 200 elastic modes over the frequency band $\mathcal{B}$ with $\nu = 1000$ frequency points in the frequency band. A damping term is added and is described by a critical damping rate of 0.01 for each elastic mode used in the reduced-order model.

6.3. Mean (or nominal) computational model prediction and comparison with the simulated experiments

(i) - Construction of the mean (or nominal) computational model. The mean (or nominal) computational model, as the predictive model of the real system defined in Section 6.2, is constructed from the designed system defined in Section 6.1. This mean computational model is made up of a damped homogeneous Timoshenko elastic beam with length $L_1 = 0.01$ m, simply supported at $x_1 = 0$ and $x_1 = 0.01$, with section $S = L_2 L_3 = 2 \times 10^{-6}$ m^2, inertia $J = L_3 L_2^3/12 = 1.6667 \times 10^{-13}$ m^4, Young's modulus $\underline{y} = 10^{10}$ N/m^2, bending stiffness $\underline{k} = J\underline{y} = 0.001667$ N×m^2, radius of gyration of the cross section $r^2 = J/S = 0.8334 \times 10^{-7}$ m^2,

mass density $1,500\,\mathrm{Kg/m}^3$, linear mass density $\rho_1 = 0.003\,\mathrm{Kg/m}$, damping rate 0.01. For integer $\alpha \geq 1$, the eigenvalues (square of the eigenfrequencies) of the Euler beam associated with the Timoshenko model are given by $\lambda_\alpha^{\mathrm{EUL}} = (\underline{k}/\rho_1)(\pi\alpha/L_1)^4$ and the corresponding eigenvalues of the Timoshenko beam model is then written as $\lambda_\alpha^{\mathrm{TIM}} = \lambda_\alpha^{\mathrm{EUL}} \times \{1 + \underline{f}_s \times (\alpha r\pi/L_1)^2\}^{-1}$ in which $\underline{f}_s = 3$ is the shear deformation factor (for a rectangular cross section) due to the effects of the shear deformation on the bending stiffness. This mean model is used to predict the transversal displacement along Ox_2 corresponding to the bending vibrations in the plane Ox_1x_2 due to the external load defined in Section 6.1 and applied to the point $x_1 = 0.0042$ (observation point P_3). There are 17 eigenfrequencies in band $]0\,,1.2]\times 10^6$ Hz and 13 eigenfrequencies in the frequency band $[1.2\,,2.2]\times 10^6$ Hz. The first six eigenfrequencies of the bending modes in plane Ox_1x_2 are 11 566 , 44 670 , 95 319 , 158 617 , 230 191 and 306 729 Hz.

(ii) - Comparison of the mean computational model prediction with the simulated experiments. The frequency response functions of the mean computational model are calculated using modal analysis with the first 30 elastic modes and in $\nu = 1000$ frequency points of band $\mathcal{B}$. We then have $n = 30$. Figure 3 displays the modulus of the frequency response function in $\log_{10}$ scale for the transversal displacement (x_2-direction) at observation point P_2 located in the neutral line with $x_1 = 0.0029$ m. In this figure, the experimental frequency response function allows the low-frequency band $\mathcal{B}_{\mathrm{LF}}$ and the medium-frequency band $\mathcal{B}_{\mathrm{MF}}$ to be defined. Using the explanations given in Section 4.1, it can be seen that these two bands can be defined as $\mathcal{B}_{\mathrm{LF}} =]0\,,3.6]\times 10^5$ Hz and $\mathcal{B}_{\mathrm{MF}} =]3.6\,,12.0]\times 10^5$ Hz. Fig. 3 shows the comparison between the mean computational

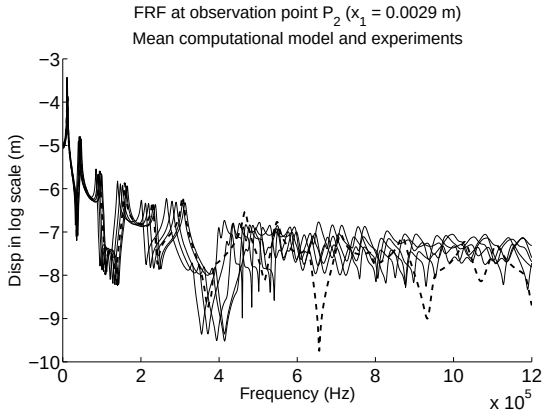

Figure 3: Modulus of the FRF in $\log_{10}$ scale over band $\mathcal{B} = \mathcal{B}_{\mathrm{LF}} \cup \mathcal{B}_{\mathrm{MF}}$ for transversal displacement at observation point P_2: experiments (five thin solid lines), mean computational model (thick dashed line).

model prediction and the simulated experiments. It can be seen, that there are significant differences due to uncertainties in the medium-frequency band $\mathcal{B}_{\mathrm{MF}}$ while in the low-frequency band $\mathcal{B}_{\mathrm{LF}}$, the predictions are very good for the first two resonances and acceptable for the next four resonances. The deterministic mean computational model has not the capability to represent the variabilities of the experiments. This figure clearly shows that system-parameter uncertainties and model uncertainties induced by modeling errors have to be taken into account in order to improve the capability of the mean computational model to predict the simulated experiments.

6.4. Identification of the optimal prior stochastic models of uncertainties

(i) - Step 1 presented in Section 4.4 is used for the identification in medium-frequency band $\mathcal{B}_{\rm MF}$. The observations used for this identification step are the $N = 6$ transversal displacements in x_2-direction at points P_1 to P_6 defined in Section 6.1. Band $\mathcal{B}_{\rm LF}$ is sampled with 300 frequency points and $\mathcal{B}_{\rm MF}$ with 700 frequency points. We then have $k_1 = 301$ and then, $N_{\rm obs} = N \times (\nu - k_1 + 1) = 6 \times 700 = 4,200$. The Monte Carlo method is carried out with $\nu_{\rm P} = 1,000$ and $\nu_{\rm NP} = 1,500$ that is to say with $1,500,000$ independent realizations of the prior stochastic models of uncertainties. We have $n = 30$. For the prior stochastic model of model uncertainties, it is assumed that only the stiffness operator is uncertain. We then have $\delta_M = \delta_D = 0$ and $\delta_K \in]0\,,0.94[$. The optimization problem defined by Eq. (39) is solved by the trial method using the estimator computed with Eq. (40) and yields $\boldsymbol{\delta}_G^{\rm opt} = (0\,,0\,,0.35)$ which means that $\delta_K = 0.35$.

(ii) - Step 2 presented in Section 4.5 is used for the identification in low-frequency band $\mathcal{B}_{\rm LF}$. The observations used for this identification step are the first $N_{\rm eig} = 6$ random eigenfrequencies in low-frequency band $\mathcal{B}_{\rm LF}$, for which the corresponding ranks of the experimental eigenfrequencies are respectively 1, 3, 6, 10, 14 and 17. The uncertain system parameters are the Young modulus $\underline{y}$ and the shear deformation factor $\underline{f}_s$ which are modeled by random variables Y and F_s respectively. The prior stochastic models of Y and F_s are constructed using the maximum entropy principle under the constraints defined by the available information which yields Gamma distributions with mean values $\underline{y} = 10^{10}$ N/m^2 and $\underline{f}_s = 3$ and with coefficients of variation δ_Y and δ_{F_s}. We then have $\mathbf{X} = (Y, F_s)$, $\underline{\mathbf{x}} = (\underline{y}, \underline{f}_s)$ and $\boldsymbol{\delta}_X = (\delta_Y, \delta_{F_s})$. For $\boldsymbol{\delta}_G = \boldsymbol{\delta}_G^{\rm opt}$ estimated in Step 1, the optimal values $(\underline{\mathbf{x}}^{\rm opt}, \boldsymbol{\delta}_X^{\rm opt})$ of $(\underline{\mathbf{x}}, \boldsymbol{\delta}_X)$ are estimated solving the optimization problem defined by Eq. (44) by the trial method and yields $\underline{\mathbf{x}}^{\rm opt} = (10^{10}, 3.8)$ and $\boldsymbol{\delta}_X^{\rm opt} = (0.12\,, 0.08)$.

(iii) - Step 3 presented in Section 4.6 is used for the identification of the posterior stochastic model of system-parameter uncertainties using the Bayes method. The optimal prior stochastic models of uncertainties which have been estimated in Steps 1 and 2 are used. We have always $\nu_{\rm P} = 1,000$ and $\nu_{\rm NP} = 1,500$. Figs. 4 and 5 display the optimal prior probability density function and the posterior probability density function of the random Young modulus Y and the random shear deformation factor F_s.

(iv) - Response predicted with the optimal prior stochastic models of uncertainties. Fig. 6 displays the confidence region of the modulus of the FRF in $\log_{10}$ scale over band $\mathcal{B} = \mathcal{B}_{\rm LF} \cup \mathcal{B}_{\rm MF}$ for transversal displacement along x_2 at observation point P_2 located in the neutral line with $x_1 = 0.0029$ m. This figure compares the experimental frequency response functions with the confidence region for $P_c = 0.95$ calculated with the stochastic reduced-order computational model using the optimal prior stochastic model of system-parameter uncertainties (Step 2) and the optimal prior stochastic model of model uncertainties (Step 1). It can be seen that the prediction of the stochastic model is good in the medium-frequency band. Fig. 7 (which is a zoom of Fig. 6 for the low-frequency band $\mathcal{B}_{\rm LF}$) shows a reasonable good prediction in this band $\mathcal{B}_{\rm LF}$. This prediction will be improved with the posterior stochastic model of system-parameter uncertainties.

(v) - Response predicted with the posterior stochastic model of system-parameter uncertainties and the optimal prior stochastic model of model uncertainties. Fig. 8 is related to the frequency

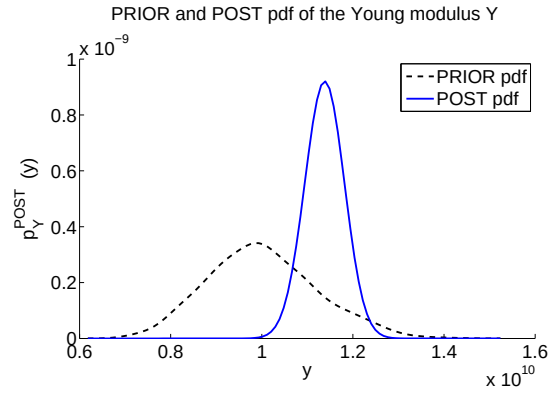

Figure 4: Optimal prior pdf (dashed line) and posterior pdf (solid line) of the random Young modulus Y.

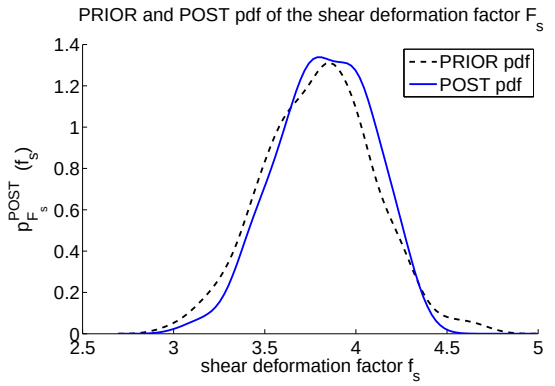

Figure 5: Optimal prior pdf (dashed line) and posterior pdf (solid line) of the random shear deformation factor F_{ξ}.

response function calculated with the stochastic reduced-order computational model using the posterior stochastic model of system-parameter uncertainties (Step 3) and the optimal prior stochastic model of model uncertainties (Step 1). This figure displays the confidence region for $P_c = 0.95$ of the modulus of the FRF in $\log_{10}$ scale over band $\mathcal{B} = \mathcal{B}_{\rm LF} \cup \mathcal{B}_{\rm MF}$, for transversal displacement along x_2 at observation point P_2 located in the neutral line with $x_1 = 0.0029$ m. It can be seen that the prediction of the stochastic model is good in the medium-frequency band. Fig. 9 (zoom of Fig. 8 for band $\mathcal{B}_{\rm LF}$) shows that the prediction has been improved in band $\mathcal{B}_{\rm LF}$.

6.5. Quality assessment

Figs. 10 to 13 are related to the quality assessment analysis. These figures display the modulus of the FRF in $\log_{10}$ scale (over band $\mathcal{B} = \mathcal{B}_{\rm LF} \cup \mathcal{B}_{\rm MF}$ for Figs. 10 and 12, and over band $\mathcal{B}_{\rm LF}$ for Figs. 11 and 13), for transversal displacement at quality assessment point QA_3 located in the neutral line with $x_1 = 0.0057$ m. The confidence region for $P_c = 0.95$ is calculated with with the stochastic reduced-order computational model using the optimal prior stochastic model (Figs. 10

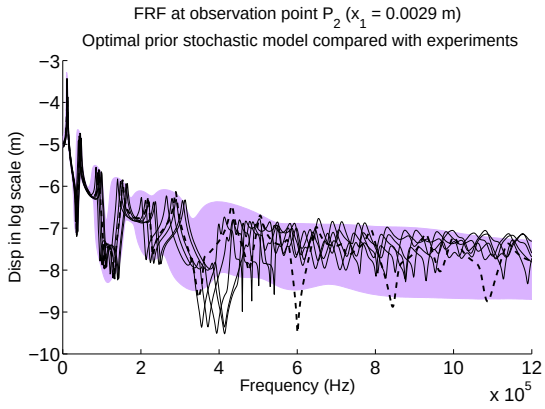

Figure 6: Confidence region of the modulus of the FRF in $\log_{10}$ scale over band $\mathcal{B} = \mathcal{B}_{\rm LF} \cup \mathcal{B}_{\rm MF}$ for transversal displacement at observation point P_2: stochastic reduced-order computational model with the optimal prior stochastic model of uncertainties (colored region), experiments (five thin solid lines), mean computational model (thick dashed line).

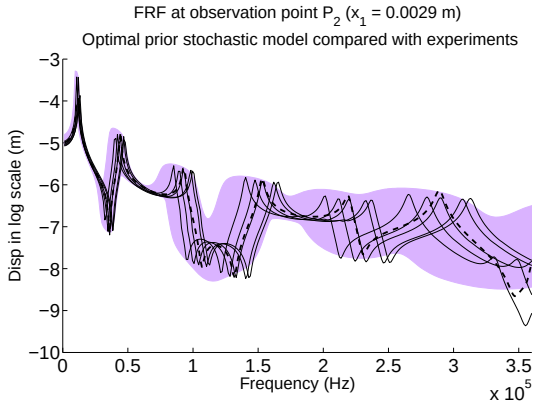

Figure 7: Zoom of Fig. 6 over the low-frequency band - Confidence region of the modulus of the FRF in $\log_{10}$ scale over band $\mathcal{B}_{\rm LF}$ for transversal displacement at observation point P_2: stochastic reduced-order computational model with the optimal prior stochastic model of uncertainties (colored region), experiments (five thin solid lines), mean computational model (thick dashed line).

and 11) and the posterior stochastic model (Figs. 12 and 13) of system-parameter uncertainties (Step 3) and the optimal prior stochastic model of model uncertainties (Step 1). It can be seen a good prediction with the optimal prior stochastic model of uncertainties, which is improved in low-frequency band $\mathcal{B}_{\rm LF}$ with the posterior stochastic model of system-parameter uncertainties in presence of the optimal prior stochastic model of model uncertainties.

7. Conclusion

A complete methodology has been presented to identify the stochastic model of uncertainties in computational structural dynamics in the low- and medium-frequency ranges. The first eigen-

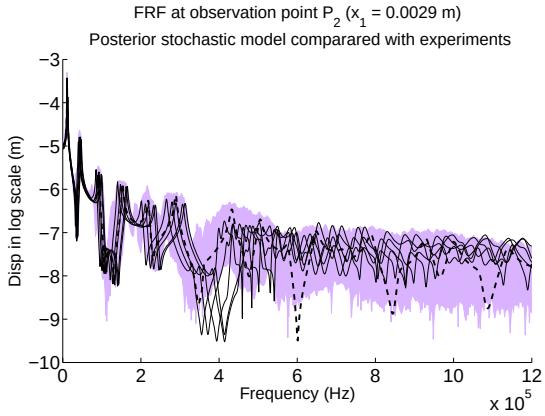

Figure 8: Confidence region of the modulus of the FRF in $\log_{10}$ scale over band $\mathcal{B} = \mathcal{B}_{\mathrm{LF}} \cup \mathcal{B}_{\mathrm{MF}}$ for transversal displacement at observation point P_2: stochastic reduced-order computational model with the posterior stochastic model of uncertainties (colored region), experiments (five thin solid lines), mean computational model (thick dashed line).

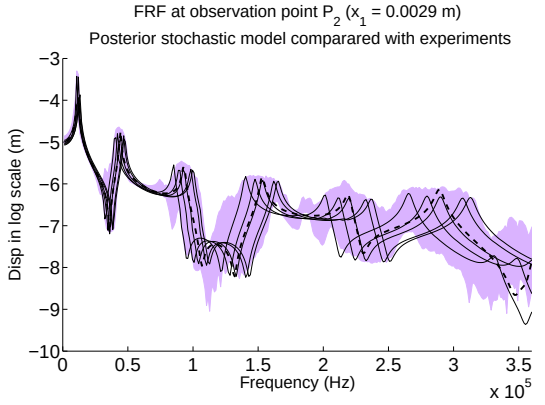

Figure 9: Zoom of Fig. 8 over the low-frequency band - Confidence region of the modulus of the FRF in $\log_{10}$ scale over band $\mathcal{B}_{\mathrm{LF}}$ for transversal displacement at observation point P_2: stochastic reduced-order computational model with the posterior stochastic model of uncertainties (colored region), experiments (five thin solid lines), mean computational model (thick dashed line).

frequencies are used to identify the stochastic model of uncertainties in the low-frequency band while the frequency response functions are used to identify it in the medium-frequency band. The system-parameter uncertainties are taken into account with the parametric probabilistic approach. The model uncertainties induced by modeling errors are taken in to account with the nonparametric probabilistic approach. The optimal prior stochastic model of model uncertainties is first identified using the frequency response functions in the medium-frequency band without taking into account the system-parameter uncertainties. Then, in presence of these optimal prior stochastic model of model uncertainties, the optimal prior stochastic model of system-parameter uncertainties is identified using the first eigenfrequencies in the low-frequency band and not the frequency response functions. Finally, always in presence of the optimal prior stochastic model of model

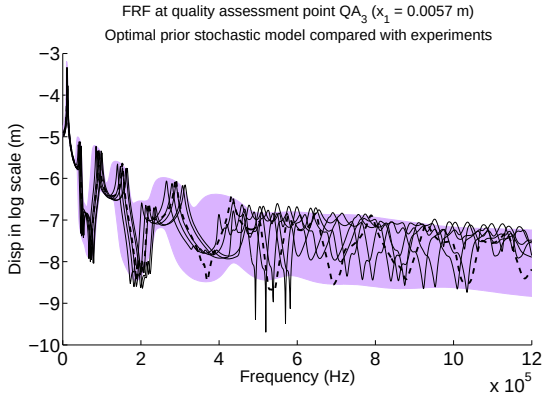

Figure 10: Confidence region of the modulus of the FRF in $\log_{10}$ scale over band $\mathcal{B} = \mathcal{B}_{\mathrm{LF}} \cup \mathcal{B}_{\mathrm{MF}}$ for transversal displacement at quality assessment point QA_3: stochastic reduced-order computational model with the optimal prior stochastic model of uncertainties (colored region), experiments (five thin solid lines), mean computational model (thick dashed line).

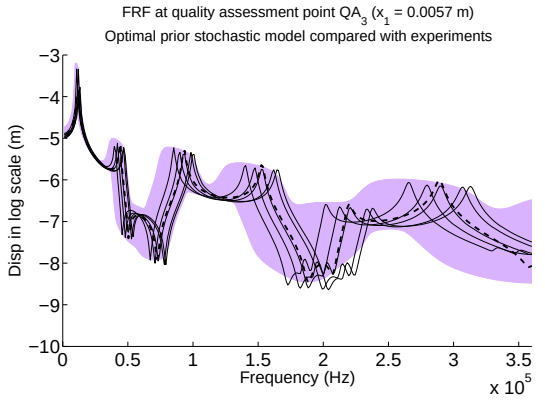

Figure 11: Zoom of Fig. 10 over the low-frequency band - Confidence region of the modulus of the FRF in $\log_{10}$ scale over band $\mathcal{B}_{\mathrm{LF}}$ for transversal displacement at quality assessment point QA_3: stochastic reduced-order computational model with the optimal prior stochastic model of uncertainties (colored region), experiments (five thin solid lines), mean computational model (thick dashed line).

uncertainties, the posterior stochastic model of system-parameter uncertainties is identified using the Bayes method and the same first eigenfrequencies belonging to the low-frequency band for which the optimal prior stochastic model has previously been identified. All the formulas required for solving such statistical inverse problems have been given. The presented application is a simple structure but which is very interesting because the mean computational model introduced significant modeling errors which play an important role in the medium-frequency band. In contrast, the behavior of the frequency response functions in low-frequency band is driven by the resonances which mainly depend on the system parameters which control the location of the first eigenfrequencies. It has been shown that a very good prediction can be obtained in the low-frequency band with the posterior stochastic model of system-parameter uncertainties while there

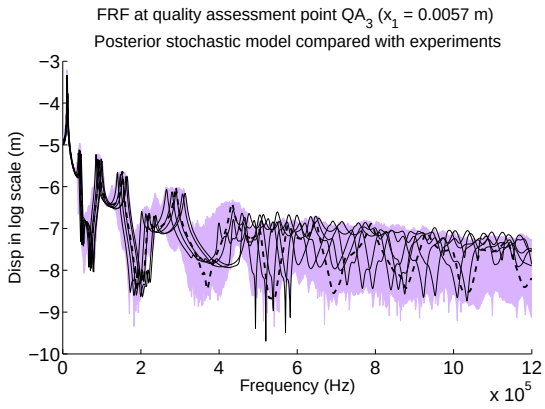

Figure 12: Confidence region of the modulus of the FRF in $\log_{10}$ scale over band $\mathcal{B} = \mathcal{B}_{\mathrm{LF}} \cup \mathcal{B}_{\mathrm{MF}}$ for transversal displacement at quality assessment point QA_3: stochastic reduced-order computational model with the posterior stochastic model of uncertainties (colored region), experiments (five thin solid lines), mean computational model (thick dashed line).

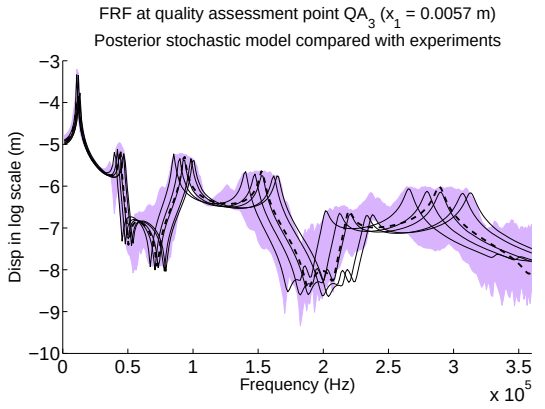

Figure 13: Zoom of Fig. 12 over the low-frequency band - Confidence region of the modulus of the FRF in $\log_{10}$ scale over band $\mathcal{B}_{\mathrm{LF}}$ for transversal displacement at quality assessment point QA_3: stochastic reduced-order computational model with the posterior stochastic model of uncertainties (colored region), experiments (five thin solid lines), mean computational model (thick dashed line).

is also a very good prediction in the medium-frequency range using the optimal prior stochastic model of modeling errors. Consequently, a posterior stochastic model is not really required for the medium-frequency band. This is an important conclusion. it should be noted that, if such a posterior stochastic model had to be built by the Bayes method for the medium-frequency range, then it would not be a problem in theory, but would pose significant challenges in terms of implementation because the random matrices introduced by the nonparametric probabilistic approach of model uncertainties are described using a large number of independent random variables.

Acknowledgement

This research was supported by the "Agence Nationale de la Recherche", Contract TYCHE, ANR-2010-BLAN-0904.

Appendix A. Random matrix theory for the nonparametric stochastic model of uncertainties

Appendix A.1. Ensemble SG_0^+ of random matrices

The Gaussian Orthogonal Ensemble (GOE) [49] cannot be used when positiveness property and integrability of the inverse are required. Consequently, adapted ensembles of random matrices have been introduced for the nonparametric probabilistic approach of uncertainties in computational structural dynamics.

The construction of the ensemble SG_0^+ of random matrices $[\mathbf{G}_0]$, defined on the probability space $(\Theta, \mathcal{T}, \mathcal{P})$, with values in the set $\mathbb{M}_n^+(\mathbb{R})$ of all the positive-definite symmetric $(n \times n)$ real matrices, and such that $E\{[\mathbf{G}_0]\} = [I_n]$ and $E\{\log(\det[\mathbf{G}_0])\} = c$ with $|c| < +\infty$, is given in [70, 71]. The dispersion of the stochastic model of random matrix $[\mathbf{G}_0]$ is controlled by the dispersion parameter δ defined by

$$\delta = \left\{ \frac{1}{n} E\{ \| [\mathbf{G}_0] - [I_n] \|_F^2 \} \right\}^{1/2} \quad , \tag{A.1}$$

which can be such that $0 < \delta < (n+1)^{1/2}(n+5)^{-1/2}$. It should be noted that $\{[\mathbf{G}_0]_{jk}, 1 \leq j \leq k \leq n\}$ are dependent random variables and it is proven in [71] that $E\{\|[\mathbf{G}_0]^{-1}\|_F^2\} < +\infty$. In addition, if $(n+1)/\delta^2$ is an integer, then this stochastic modeling coincides with the Wishart probability distribution [4, 70].

The generator of independent realizations (which is required to solve the random equations with the Monte Carlo method) is detailed in [70, 71].

Appendix A.2. Ensemble SG_ε^+ of random matrices

Let $0 \leq \varepsilon \ll 1$ be a positive number as small as one wants. The ensemble $\mathrm{SG}_\varepsilon^+$ is defined as the ensemble of all the random matrices such that

$$[\mathbf{G}] = \frac{1}{1+\varepsilon} \{ [\mathbf{G}_0] + \varepsilon [I_n] \} \quad , \tag{A.2}$$

in which $[\mathbf{G}_0]$ is a random matrix which belongs to ensemble SG_0^+. Let $[\mathbf{G}]$ be in $\mathrm{SG}_\varepsilon^+$ (if $\varepsilon = 0$, then $\mathrm{SG}_\varepsilon^+ = \mathrm{SG}_0^+$ and $[\mathbf{G}] = [\mathbf{G}_0]$). It can easily be seen that $E\{[\mathbf{G}]\} = [I_n]$ and that, for all second-order random variable $\mathbf{X}$, defined on the probability space $(\Theta, \mathcal{T}, P)$, with values in $\mathbb{R}^n$, we have $E\{< [\mathbf{G}]\,\mathbf{X}, \mathbf{X} >\} \geq c_\varepsilon E\{\|\mathbf{X}\|^2\}$ in which $c_\varepsilon = \varepsilon/(1+\varepsilon)$, where $<\mathbf{x}, \mathbf{y}>= \sum_j x_j y_j$ is the Euclidean inner product of the vectors $\mathbf{x}$ and $\mathbf{y}$, and where $\|\mathbf{x}\|$ is the associated Euclidean norm. Finally, for all $\varepsilon \geq 0$, it can also be proven that $E\left\{\|[\mathbf{G}]^{-1}\|_F^2\right\} < +\infty$.

References

[1] D. Amsallem, C. Farhat, Interpolation method for adapting reduced-order models and application to aeroelsaticity, *AIAA Journal*, 46(7) (2008) 1803-1813.

[2] D. Amsallem, J. Cortial, K. Carlberg, C. Farhat, A method for interpolating on manifolds structural dynamics reduced-order models, *International Journal for Numerical Methods in Engineering*, 80(9) (2009) 1241-1258.

[3] D. Amsallem, C. Farhat, An online method for interpolating linear parametric reduced-order models, *SIAM Journal on Scientific Computing*, 33(5) (2011) 2169-2198.
[4] T. W. Anderson, *Introduction to Multivariate Statistical Analysis*, John Wiley & Sons, New York, 1958.
[5] M. Arnst, D. Clouteau, H. Chebli, R. Othman, G. Degrande, A nonparametric probabilistic model for ground-borne vibrations in buildings, *Probabilistic Engineering Mechanics*, 21(1) (2006) 18-34.
[6] M. Arnst, D. Clouteau, M. Bonnet, Inversion of probabilistic structural models using measured transfer functions, *Computer Methods in Applied Mechanics and Engineering* 197(6-8) (2008)589-608.
[7] A. Batou, C. Soize, Experimental identification of turbulent fluid forces applied to fuel assemblies using an uncertain model and fretting-wear estimation, *Mechanical Systems and Signal Processing* 23(7) (2009) 2141-2153.
[8] A. Batou, C. Soize, M. Corus, Experimental identification of an uncertain computational dynamical model representing a family of structures, *Computer and Structures* 89(13-14) (2011) 1440-1448.
[9] J.L. Beck, L.S. Katafygiotis, Updating models and their uncertainties. I: Bayesian statistical framework, *Journal of Engineering Mechanics* 124(4) (1998) 455-461.
[10] J.L. Beck, E. Chan, A. Irfanoglu, C. Papadimitriou, Multi-criteria optimal structural design under uncertainty, *Earthquake Engineering and Structural Dynamics* 28(7) (1999) 741-761.
[11] J.L. Beck, S.K. Au, Bayesian updating of structural models and reliability using Markov chain Monte Carlo simulation, *Journal of Engineering Mechanics - ASCE* 128(4) (2002) 380-391.
[12] J.L. Beck, Bayesian system identification based on probability logic, *Structural Control and Health Monitoring* 17(7) (2010) 825-847.
[13] J. S. Bendat, A. G. Piersol, *Random Data: Analysis and Measurement Procedures*, John Wiley & Sons, New York, 1971.
[14] J. S. Bendat, A. G. Piersol, *Engineering Applications of Correlation and Spectral Analysis*, John Wiley & Sons, New York, 1980.
[15] J. M. Bernardo, A. F. M. Smith, *Bayesian Theory*, John Wiley & Sons, Chichester, 2000.
[16] A.W. Bowman, A. Azzalini, *Applied Smoothing Techniques for Data Analysis*, Oxford University Press, 1997.
[17] E. Capiez-Lernout, C. Soize, J.-P. Lombard, C. Dupont, E. Seinturier, Blade manufacturing tolerances definition for a mistuned industrial bladed disk, *Journal of Engineering for Gas Turbines and Power* 127(3) (2005) 621-628.
[18] E. Capiez-Lernout, M. Pellissetti, H. Pradlwarter, G. I. Schueller, C. Soize, Data and model uncertainties in complex aerospace engineering systems, *Journal of Sound and Vibration* 295(3-5) (2006) 923-938.
[19] E. Capiez-Lernout, C. Soize, Robust design optimization in computational mechanics, *Journal of Applied Mechanics - Transactions of the ASME* 75(2) (2008), 021001-1-11.
[20] E. Capiez-Lernout, C. Soize, Robust updating of uncertain damping models in structural dynamics for low- and medium-frequency ranges, *Mechanical Systems and Signal Processing* 22(8) (2008) 1774-1792.
[21] E. Capiez-Lernout, C. Soize, M. Mignolet, Computational stochastic statics of an uncertain curved structure with geometrical nonlinearity in three-dimensional elasticity, *Computational Mechanics*, 49(1) (2012) 87-97.
[22] B.P. Carlin, T.A. Louis, *Bayesian Methods for Data Analysis*, Third Edition, CRC Press, Boca Raton, 2009.
[23] H. Chebli, C. Soize, Experimental validation of a nonparametric probabilistic model of non homogeneous uncertainties for dynamical systems, *Journal of the Acoustical Society of America* 115(2) (2004) 697-705.
[24] C. Chen, D. Duhamel, C. Soize, Probabilistic approach for model and data uncertainties and its experimental identification in structural dynamics: Case of composite sandwich panels, *Journal of Sound and Vibration* 294(1-2) (2006) 64-81.
[25] S.H. Cheung, J.L. Beck, Bayesian model updating using hybrid monte carlo simulation with application to structural dynamic models with many uncertain parameters, *Journal of Engineering Mechanics - ASCE* 135(4) (2009) 243-255.
[26] S.H. Cheung, J.L. Beck, Calculation of posterior probabilities for bayesian model class assessment and averaging from posterior samples based on dynamic system data, *Computer-Aided Civil and Infrastructure Engineering* 25(5) (2010) 304-321.
[27] J.Y. Ching, J.L. Beck, K.A. Porter, Bayesian state and parameter estimation of uncertain dynamical systems, *Probabilistic Engineering Mechanics* 21(1) (2006) 81-96.
[28] P. Congdon, *Bayesian Statistical Modelling, Second Edition*, John Wiley & Sons, Chichester, 2007.
[29] R. Cottereau, D. Clouteau, C. Soize, Construction of a probabilistic model for impedance matrices, *Computer Methods in Applied Mechanics and Engineering* 196(17-20) (2007) 2252-2268.
[30] G. Deodatis, P. D. Spanos (Guest Editors), 5th International Conference on computational stochastic mechanics, *Special issue of the Probabilistic Engineering Mechanics* 23(2-3) (2008) 103-346.
[31] C. Desceliers, C. Soize, Q. Grimal, M. Talmant, S. Naili, Determination of the random anisotropic elasticity layer using transient wave propagation in a fluid-solid multilayer: Model and experiments, *Journal of the Acoustical Society of America* 125(4) (2009) 2027-2034.
[32] J. Duchereau, C. Soize, Transient dynamics in structures with nonhomogeneous uncertainties induced by complex joints, *Mechanical Systems and Signal Processing*, 20(4) (2006) 854-867.

[33] J.-F. Durand, C. Soize, L. Gagliardini, Structural-acoustic modeling of automotive vehicles in presence of uncertainties and experimental identification and validation, *Journal of the Acoustical Society of America* 124(3) (2008) 1513-1525.
[34] I. Elishakoff, C. Soize (eds.), *Nondeterministic Mechanics*, CISM Courses and Lectures, vol. 539, SpringerWien-NewYork, 2012.
[35] B. Faverjon, R. Ghanem, Stochastic inversion in acoustic scattering, *Journal of the Acoustical Society of America* 119(6) (2006) 3577-3588.
[36] C. Fernandez, C. Soize, L. Gagliardini, Sound-insulation layer modelling in car computational vibroacoustics in the medium-frequency range, *Acta Acustica united with Acustica (AAUWA)* 96(3) (2010) 437-444.
[37] R. Ghanem, P.D. Spanos, *Stochastic Finite Elements: A spectral Approach*, Springer-verlag, New-York, 1991 (revised edition, Dover Publications, New York, 2003).
[38] B. Goller, H.J. Pradlwarter, G.I. Schueller, Robust model updating with insufficient data, *Computer Methods in Applied Mechanics and Engineering* 198(37-40) (2009) 3096-3104.
[39] B. Goller, G.I. Schueller, Investigation of model uncertainties in Bayesian structural model updating, *Journal of Sound and Vibration* 330(25) (2011) 6122-6136.
[40] E. T. Jaynes, Information theory and statistical mechanics, *Physical Review* 108(2) (1957) 171-190.
[41] J. Kaipio, E. Somersalo, *Statistical and Computational Inverse Problems*, Springer-Verlag, New York, 2005.
[42] M. Kassem, C. Soize, L. Gagliardini, Energy density field approach for low- and medium-frequency vibroacoustic analysis of complex structures using a stochastic computational model, *Journal of Sound and Vibration* 323(3-5) (2009) 849-863.
[43] L.S. Katafygiotis, J.L. Beck, Updating models and their uncertainties. II: Model identifiability, *Journal of Engineering Mechanics - ASCE* 124(4) (1998) 463-467.
[44] Le-Maitre OP, Knio O. Spectral Methods for Uncertainty Quantification with Applications to Computational Fluid Dynamics. Heidelberg: Springer; 2010.
[45] X. Ma, N. Zabaras, An efficient Bayesian inference approach to inverse problems based on an adaptive sparse grid collocation method, *Inverse Problems* 25(3) (2009) Article Number: 035013.
[46] R. Mace, W. Worden, G. Manson (Editors), Uncertainty in structural dynamics, *Special issue of the Journal of Sound and Vibration*, 288(3) (2005) 431-790.
[47] D.J.C. MacKay, *Information Theory, Inference and Learning Algorithms*, Cambridge University Press, Cambridge, 2003
[48] Y.M. Marzouk, H.N. Najm, L.A. Rahn, Stochastic spectral methods for efficient Bayesian solution of inverse problems, *Journal of Computational Physics*, 224(2) (2007) 560-586.
[49] M. L. Mehta, *Random Matrices, Revised and Enlarged Second Edition*, Academic Press, New York, 1991.
[50] M. P. Mignolet, C. Soize, Nonparametric stochastic modeling of linear systems with prescribed variance of several natural frequencies, *Probabilistic Engineering Mechanics*, 23(2-3) (2008) 267-278.
[51] M. P. Mignolet, C. Soize, Nonparametric stochastic modeling of structures with uncertain boundary conditions and uncertain coupling between substructures. Proceedings of LSAME.08: *Leuven Symposium on Applied Mechanics in Engineering*, edited by B. Bergen, M. De Munck, M. Desmet et al., Pts 1 and 2, pp. 539-552, Katholieke Univ Leuven (2008).
[52] M. P. Mignolet, C. Soize, Nonparametric stochastic modeling of structural dynamic systems with uncertain boundary conditions. Proceedings of the AIAA Conference 2008, Schaumburg (Chicago), Illinois, USA, pp.1-12, AIAA (2008).
[53] M. P. Mignolet, C. Soize, Stochastic reduced order models for uncertain nonlinear dynamical systems, *Computer Methods in Applied Mechanics and Engineering*, 197(45-48) (2008) 3951-3963 .
[54] Nouy A. Proper Generalized Decomposition and separated representations for the numerical solution of high dimensional stochastic problems, *Archives of Computational Methods in Engineering*, 17(4) (2010) 403-34.
[55] R. Ohayon, C. Soize, Structural Acoustics and Vibration, Academic Press, London, 1998.
[56] R. Ohayon, C. Soize, Advanced computational dissipative structural acoustics and fluid-structure interaction in low- and medium-frequency domains. Reduced-order models and uncertainty quantification, *International Journal of Aeronautical and Space Sciences*, to appear (2012).
[57] C. Papadimitriou, J.L. Beck, S.K. Au, Entropy-based optimal sensor location for structural model updating, *Journal of Vibration and Control* 6(5) (2000) 781-800.
[58] C. Papadimitriou, J.L. Beck, L.S. Katafygiotis, Updating robust reliability using structural test data, *Probabilistic Engineering Mechanics*, 16(2) (2001)103-113.
[59] M. Papadrakakis, N.D. Lagaros, Reliability-based structural optimization using neural networks and Monte Carlo simulation, *Computer Methods in Applied Mechanics and Engineering* 191(32) (2002) 3491-3507.
[60] M. Pellissetti, E. Capiez-Lernout, H. Pradlwarter, C. Soize, G. I. Schueller, Reliability analysis of a satellite structure with a parametric and a non-parametric probabilistic model, *Computer Methods in Applied Mechanics and Engineering* 198(2) (2008) 344-357.

[61] T.G. Ritto, C. Soize, R. Sampaio, Robust optimization of the rate of penetration of a drill-string using a stochastic nonlinear dynamical model, *Computational Mechanics*, 45(5) (2010) 415-427.
[62] G.I. Schueller (Editor), Computational methods in stochastic mechanics and reliability analysis, *Computer Methods in Applied Mechanics and Engineering* 194(12-16) (2005) 1251-1795.
[63] G.I. Schueller (Guest Editor), Uncertainties in structural mechanics and analysis-computational methods, *Special issue of Computer and Structures*, 83(14) (2005) 1031-1150.
[64] G.I. Schueller, On the treatment of uncertainties in structural mechanics and analysis, *Computers ans Structures* 85(5-6) (2007) 235-243.
[65] G.I. Schueller, H.A. Jensen, Computational methods in optimization considering uncertainties - An overview, *Computer Methods in Applied Mechanics and Engineering* 198(1) (2008) 2-13.
[66] G.I. Schueller, H.J. Pradlwarter, Uncertain linear systems in dynamics: Retrospective and recent developments by stochastic approaches, *Engineering Structures* 31(11) (2009) 2507-2517.
[67] G.I. Schueller, H.J. Pradlwarter, Uncertainty analysis of complex structural systems, *International Journal for Numerical Methods in Engineering* 80(6-7) (2009) 881-913.
[68] R .J. Serfling, *Approximation Theorems of Mathematical Statistics*, John Wiley & Sons, 1980.
[69] C. E. Shannon, A mathematical theory of communication, *Bell System Technology Journal*, 27(14) (1948) 379-423 & 623-659.
[70] C. Soize, A nonparametric model of random uncertainties on reduced matrix model in structural dynamics, *Probabilistic Engineering Mechanics* 15(3) (2000) 277-294.
[71] C. Soize, Maximum entropy approach for modeling random uncertainties in transient elastodynamics, *Journal of the Acoustical Society of America* 109(5) (2001)1979-1996.
[72] C. Soize, Random matrix theory and non-parametric model of random uncertainties, *Journal of Sound and Vibration* 263(4) (2003) 893-916.
[73] C. Soize, Uncertain dynamical systems in the medium-frequency range, *Journal of Engineering Mechanics* 129(9) (2003) 1017-1027.
[74] C. Soize, Random matrix theory for modeling uncertainties in computational mechanics, *Computer Methods in Applied Mechanics and Engineering* 194(12-16) (2005) 1333-1366.
[75] C. Soize, Construction of probability distributions in high dimension using the maximum entropy principle. Applications to stochastic processes, random fields and random matrices, *International Journal for Numerical Methods in Engineering* 76(10) (2008), 1583-1611.
[76] C. Soize, E. Capiez-Lernout, J.-F. Durand, C. Fernandez, L. Gagliardini, Probabilistic model identification of uncertainties in computational models for dynamical systems and experimental validation, *Computer Methods in Applied Mechanics and Engineering* 198(1) (2008) 150-163.
[77] C. Soize, E. Capiez-Lernout, R. Ohayon, Robust updating of uncertain computational models using experimental modal analysis, *AIAA Journal* 46(11) (2008) 2955-2965.
[78] C. Soize, Generalized probabilistic approach of uncertainties in computational dynamics using random matrices and polynomial chaos decompositions, *International Journal for Numerical Methods in Engineering* 81(8) (2010) 939-970.
[79] C. Soize, *Stochastic Models of Uncertainties in Computational Mechanics*, Lecture Notes in Mechanics Series, Vol. 2, Engineering Mechanics Institute (EMI) of the American Society of Civil Engineers (ASCE), Reston, VA, USA, 2012.
[80] C. Soize, I.E. Poloskov, Time-domain formulation in computational dynamics for linear viscoelastic media with model uncertainties and stochastic excitation, *Computers and Mathematics with Applications*, on line, doi:10.1016/j.camwa.2012.09.010 (2012).
[81] J.C. Spall, *Introduction to Stochastic Search and Optimization*, John Wiley and Sons,Hoboken, New Jersey, 2003.
[82] A.A. Taflanidis, J.L. Beck, An efficient framework for optimal robust stochastic system design using stochastic simulation, *Computer Methods in Applied Mechanics and Engineering* 198(1) (2008) 88-101.
[83] M.T. Tan, G.-L. Tian, K.W. Ng, *Bayesian Missing Data Problems, EM, Data Augmentation and Noniterative Computation*, Chapman & Hall / CRC Press, Boca Raton, 2010.
[84] A. Tarantola, *Inverse Problem Theory and Methods for Model Parameter Estimation*, SIAM (Society for Industrial and Applied Mathematics), Philadelphia, 2005.
[85] G. R. Terrell, D. W. Scott, Variable kernel density estimation, *The Annals of Statistics* 20(3) (1992) 1236-1265.
[86] E. Walter, L. Pronzato, *Identification of Parametric Models from Experimental Data*, Springer, 1997.
[87] J.B. Wang, N. Zabaras, A Bayesian inference approach to the inverse heat conduction problem, *International Journal of Heat and Mass Transfer* 47(17-18) (2004) 3927-3941.
[88] J.B. Wang, N. Zabaras, Hierarchical Bayesian models for inverse problems in heat conduction, *Inverse Problems* 21(1) (2005) 183-206.
[89] M. Wright, R. Weaver, *New Directions in Linear Acoustics: Random Matrix Theory, Quantum Chaos and Complexity*, Cambridge University Press, Cambridge, 2010.

[90] N. Zabaras, B. Ganapathysubramanian, A scalable framework for the solution of stochastic inverse problems using a sparse grid collocation approach, *Journal of Computational Physics*, 227(9) (2008) 4697-4735.